Compositional mapping of minor planets population using near-infrared data

Marcel Popescu

16 – Nov - 2017

Few words about Astronomical Institute of the Romanian Academy

- Astronomical Institute was founded on 1908 and it currently belongs to the Romanian Academy.
- The main building is located in Bucharest (in the Carol Park area).
- The planetary sciences group from AIRA includes: Alin Nedelcu, Ioana Boaca, Bogdan Dumitru, Radu Gherase, Adrian Sonka, Petre Paraschiv, Jad Mansour and Marcel Popescu.

Main building of Astronomical Institute - Bucharest

Why asteroids?

- About 750 000 minor planets (small bodies of the Solar System orbiting the Sun) are known today. They occupy a variety of orbits ranging from near-Earth to Kuiper Belt.

  - ~700 000 Main Belt Asteroids (MBAs); ~17 000 Near Earth Asteroids (NEAs) → 1,850 potentially hazardous asteroids (PHA)

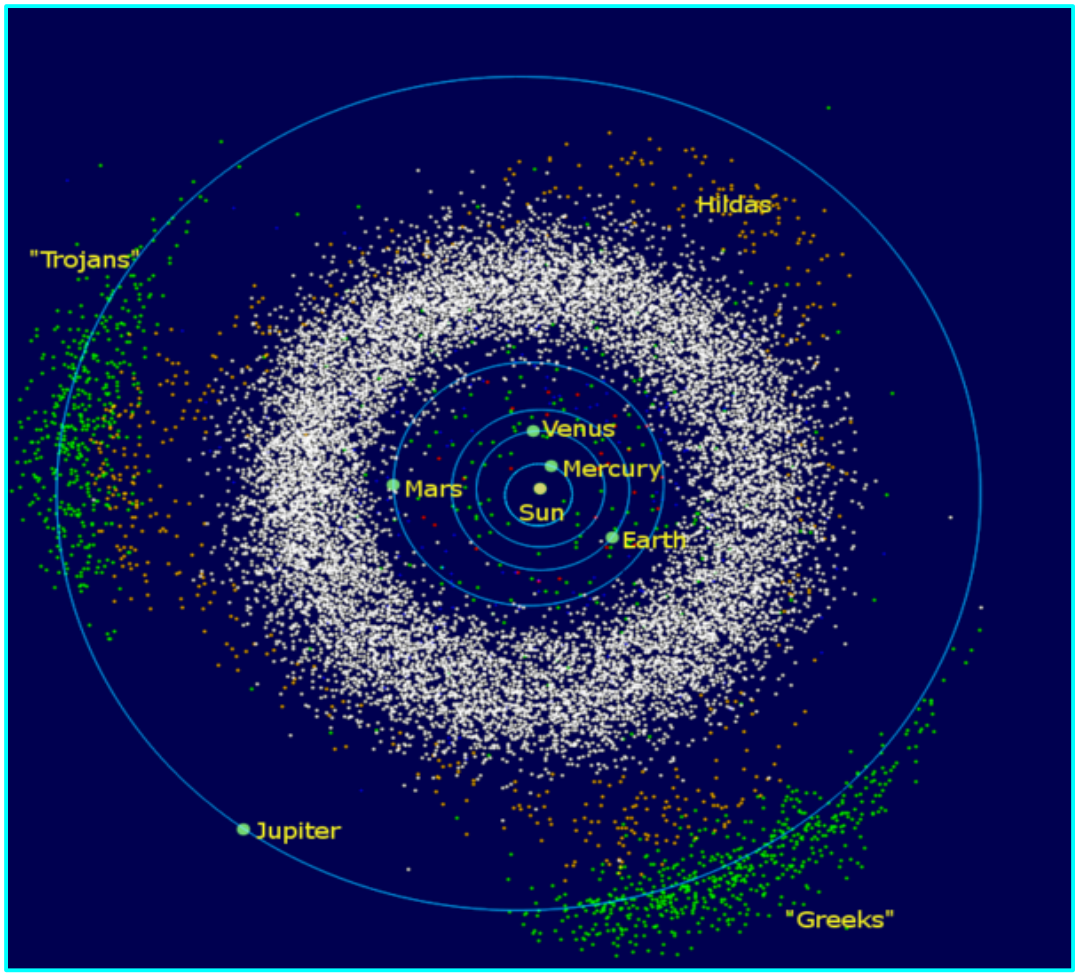

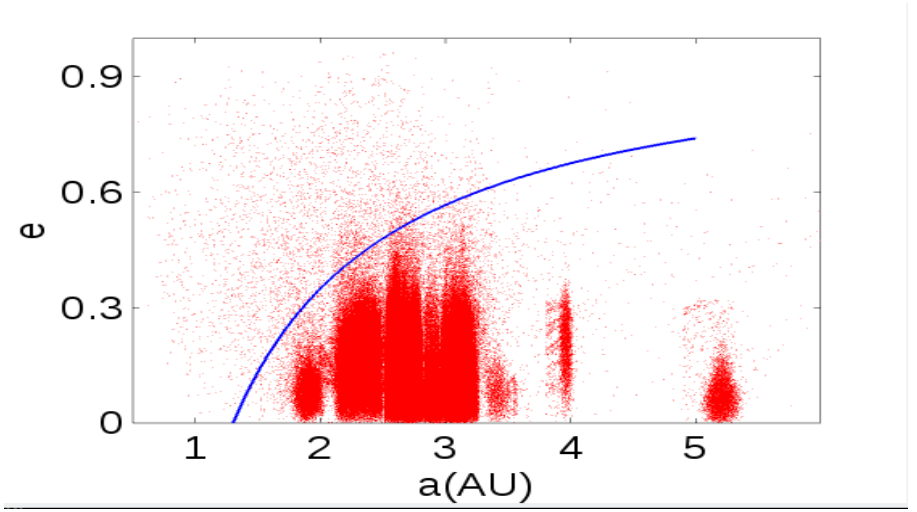

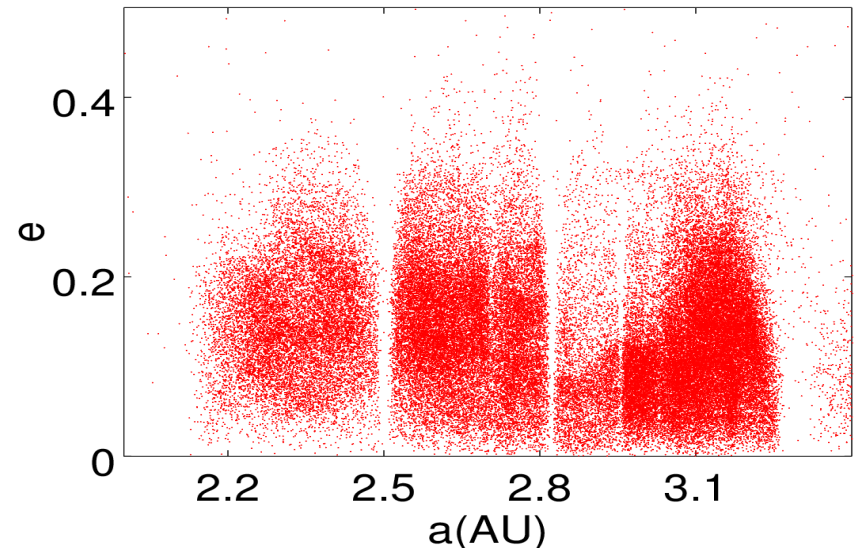

Why asteroids?

Scientific point – Key questions

- *What were the processes occurring in the early Solar System?*
- *What are the physical properties of the building blocks of terrestrial planets?*
- *Do asteroids contain pre-solar material yet unknown in meteoritic samples?*
- *How asteroids can shed light on the origin of molecules necessary for life?*

Source: M.A. Barucci 2011

- *Space exploration of asteroids (Dawn, New-Horizons, OSIRIS-REx, Hayabusa2)*
- *Groundbased studies – critical for space mission requirements;*

Practical point

- *Space situational awareness – impact to the Earth;*
- *Exploiting raw materials from asteroids.*

Hayabusa over Itokawa surface. Credit: JAXA

Finding the physical properties of asteroids

- Photometry → lightcurve → rotation period → shape
- Spectro-photometry → surface composition
- Spectroscopy → surface composition
- Radar → shape, albedo, rotation period
- Polarimetry → surface properties (texture)

Note: Telescope observations are limited by the atmosphere absorption

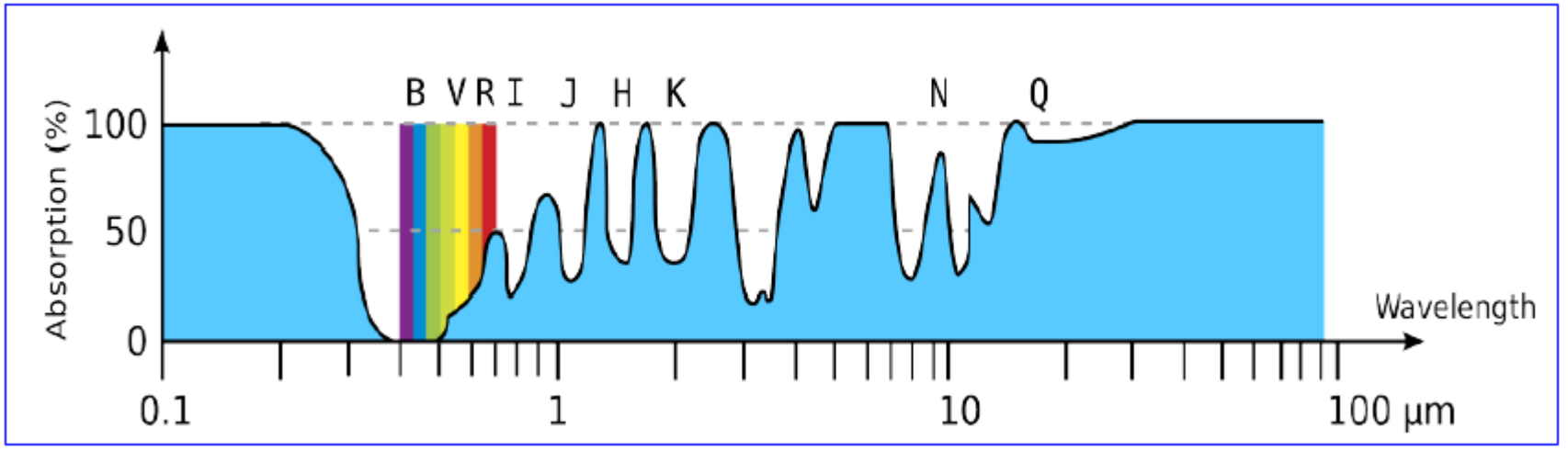

Source: Carry, Ph.D. Thesis

Reflexion vs Emission

The radiation received from the Sun by an airless body:

- *Absorbed radiation – heating the body;*
- ***Reflected radiation.***

$$Y(\lambda) = [X(\lambda) \cdot HA(\lambda) + T(\lambda)] \cdot HT(\lambda)$$

- *Y (λ) - the radiation flux recorded by the spectrometer;*
- *X(λ) - the radiation flux from the Sun;*
- *HA(λ) - the transfer function of the asteroid;*
- *T (λ) - the thermal infrared emission of the asteroid.*
- *HT (λ) include the transfer function of the Earth atmosphere and of optical instrument;`*

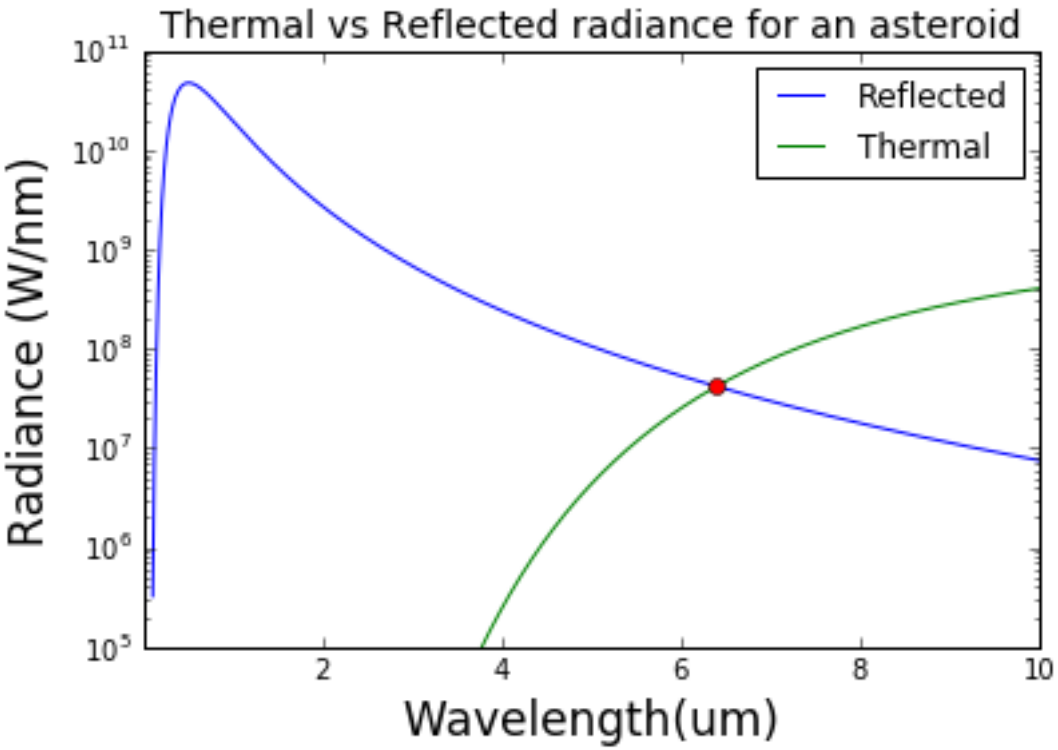

Example: getting a spectrum

Asteroid spectrum

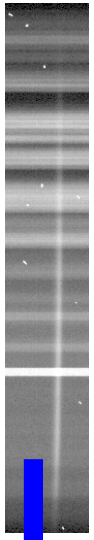

Calibration using He-Ar lamp

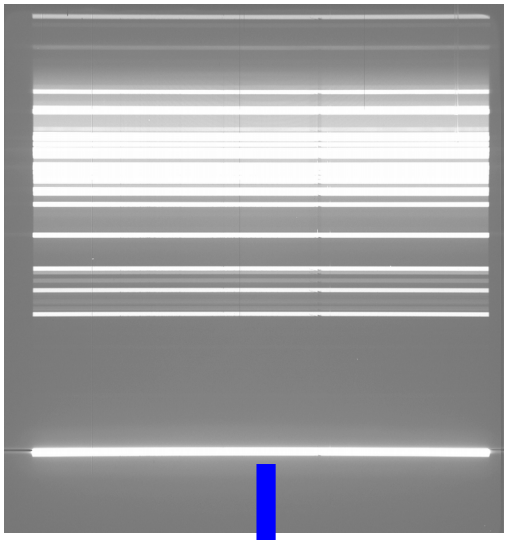

Solar analog spectrum

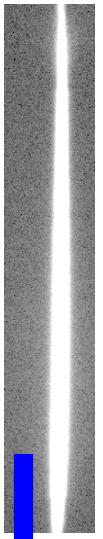

Raw spectrum

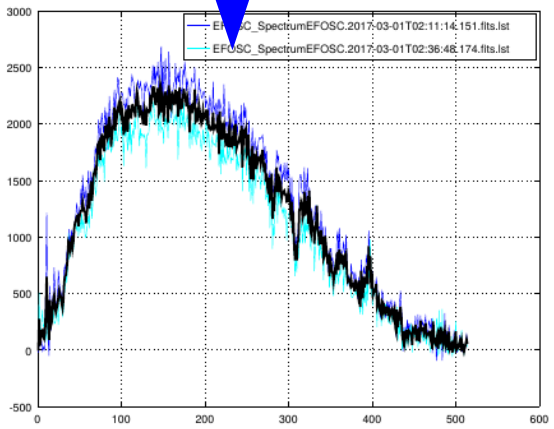

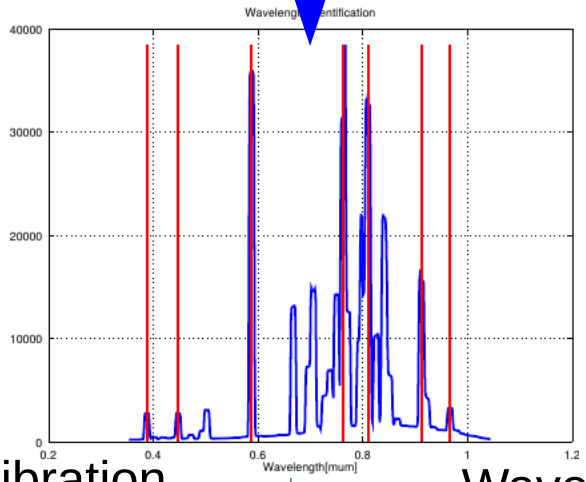

Raw spectrum

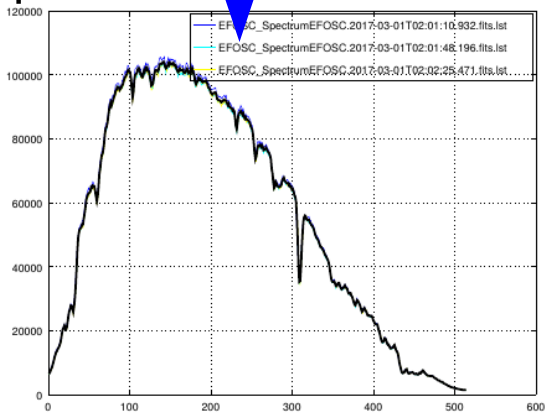

Wavelength calibration

Wavelength calibration

Division with the solar analog

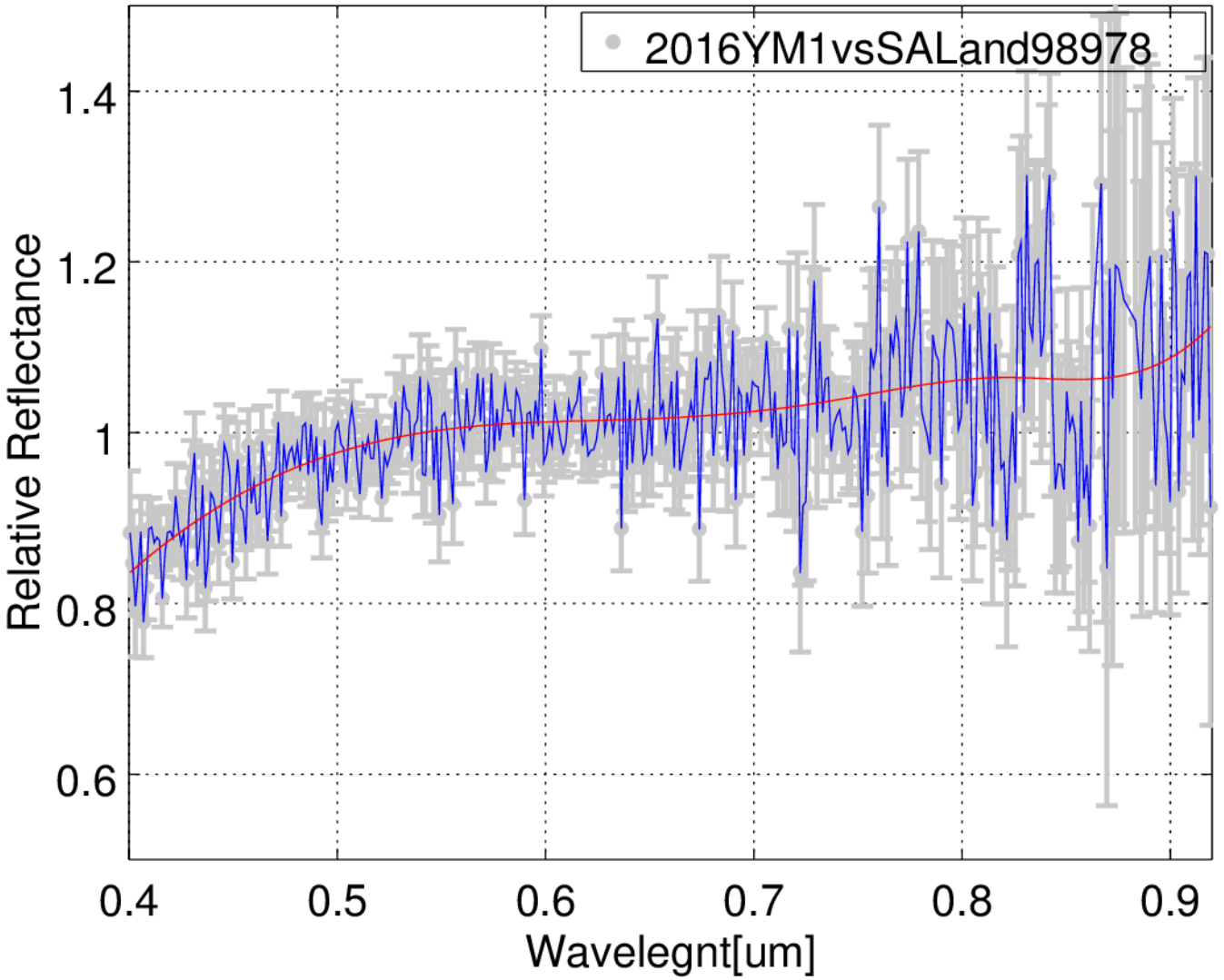
2016YM1vsSALand98978
Relative Reflectance
1.4
1.2
1
0.8
0.6
0.4
0.5
0.6
0.7
0.8
0.9
Wavelegnt[um]

The surface composition of minor planets

Astronomy ← spectroscopy → fundamental physics

The surface properties of an asteroid can be inferred through spectral and spectro - photometric measurements at wavelengths from the ultraviolet (UV) to the infrared.

- Comparative planetology;
- Taxonomy;
- Mineralogical models.

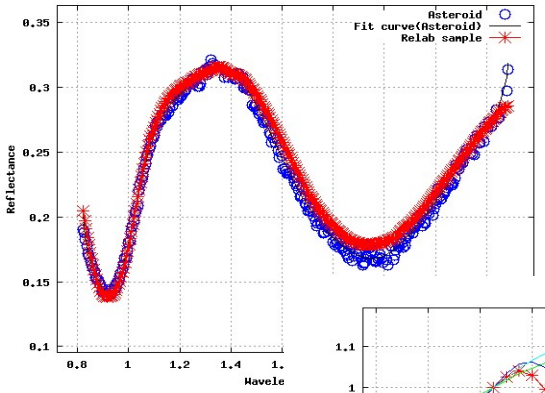

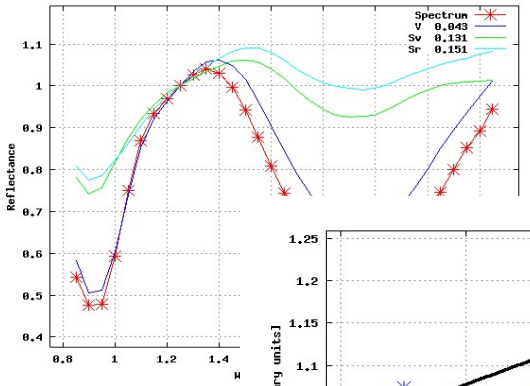

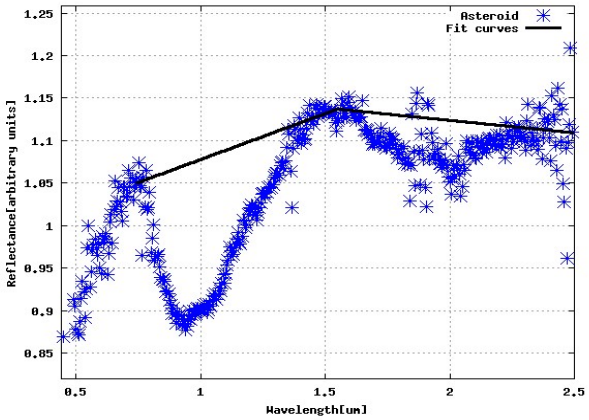

Taxonomy and comparative planetology

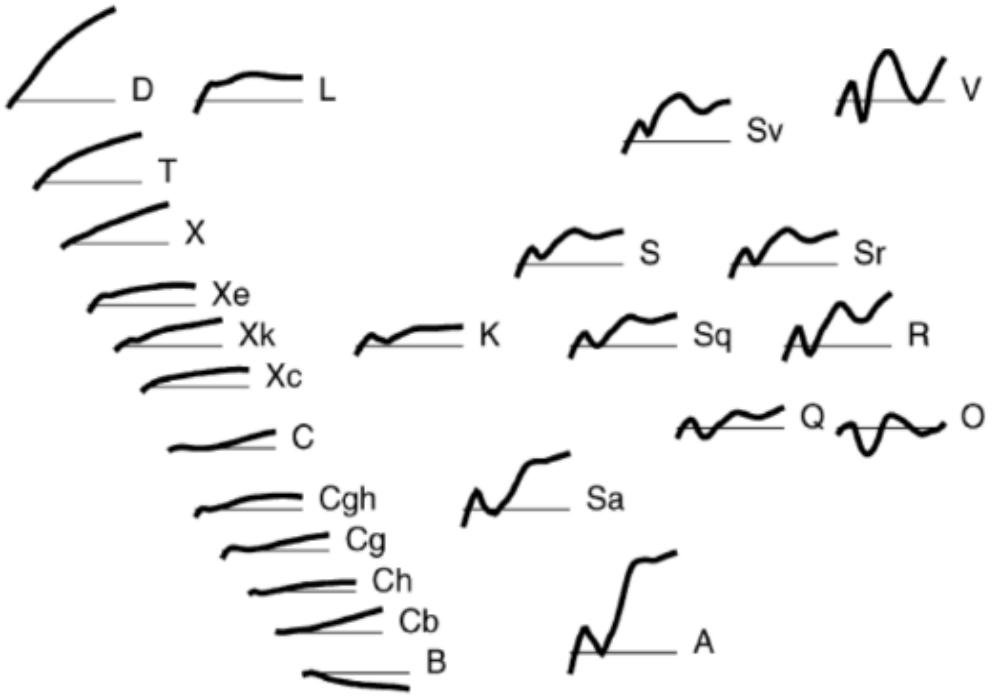

The 24 spectral classes of the Bus-DeMeo taxonomy key measured over visible and near-infrared wavelengths (0.45 -2.45 um) (DeMeo et al.,2009)

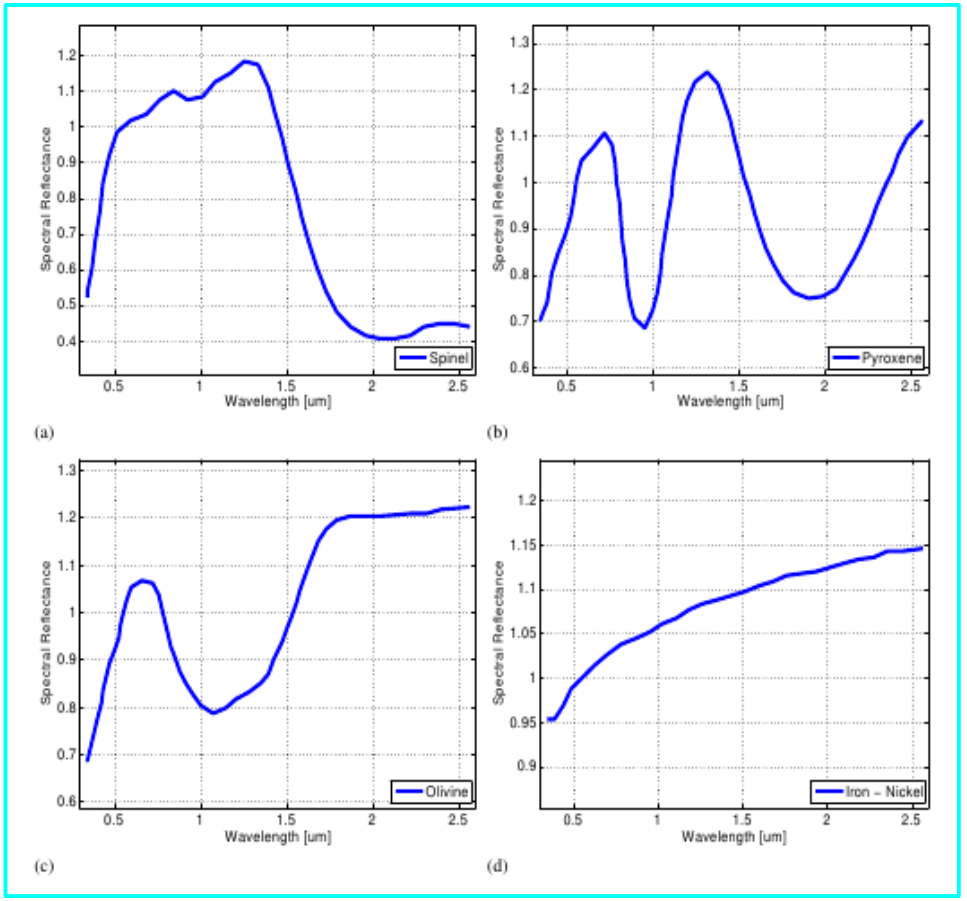

a) Spinel, b) Pyroxene, c) Olivine, d) Iron-Nickel

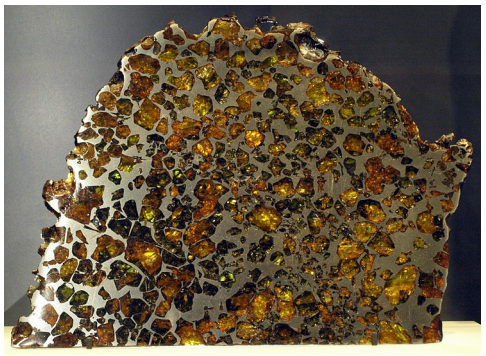

Meteorites. Source Internet

Case study 1: asteroids associated with Taurid meteor shower

- We investigated the surface mineralogy of the asteroids associated with Taurid Complex using visible and near-infrared spectral data.

- (2201) Oljato,(4183) Cuno, (4486) Mithra, (5143) Heracles, and (6063) Jason, -> spectral characteristics similar to the S complex with spectral bands around 1 and 2 μm.

- (269690) 1996 RG3 - a primitive C-type object supporting the hypothesis of a common origin with the comet P/Encke.

- - Madiedo et al. 2014 found that five bright Taurid fireballs observed between 2010 and 2012, had spectra compatible with a chondritic composition.

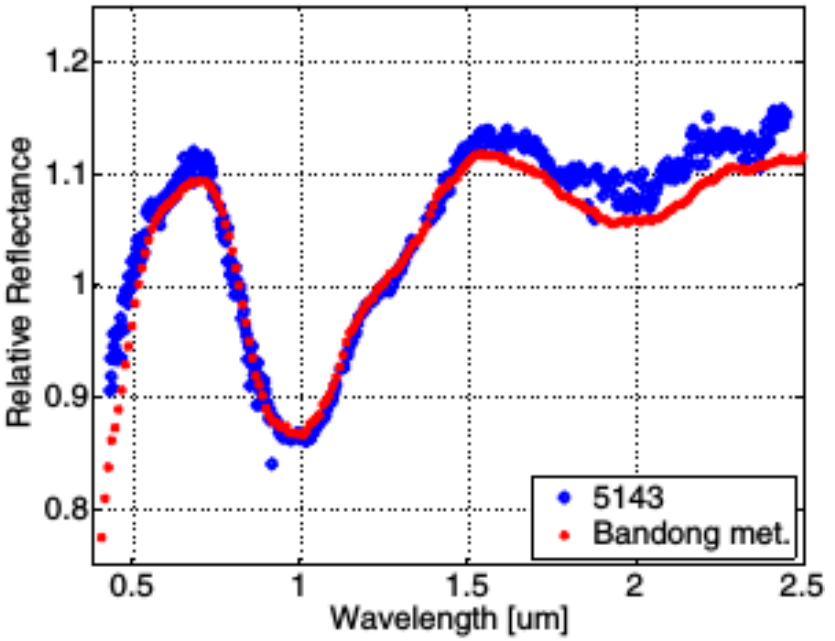

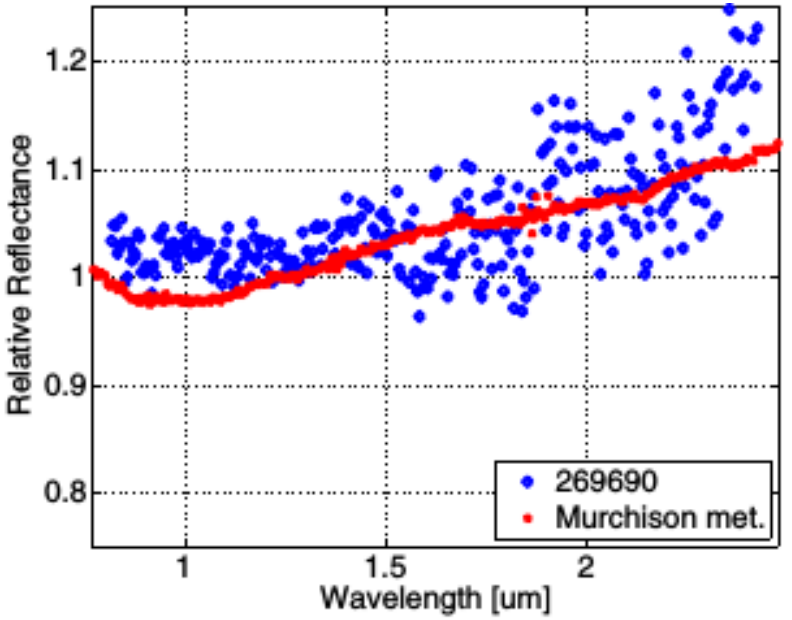

Popescu et.al; A&A, 2014

Case study 2: Spectral properties of near-Earth asteroids on cometary orbits

The asteroids in cometary orbits (ACOs) are observationally asteroids and dynamically comets.

The active, dormant and dead comets are very dark, often reddish, objects , with spectra similar to B, D, P, and C-type asteroids of the outer Solar System with albedo and colors probably controlled by carbonaceous dust containing reddish organic compounds.

Near-Earth asteroids with TJ<3 cover a wide spectral diversity

The taxonomic distribution is dominated by S-types for TJ~2.9 and by primitive types for TJ<2.8

0.5 - 8 % end-state comets are in the NEAs population

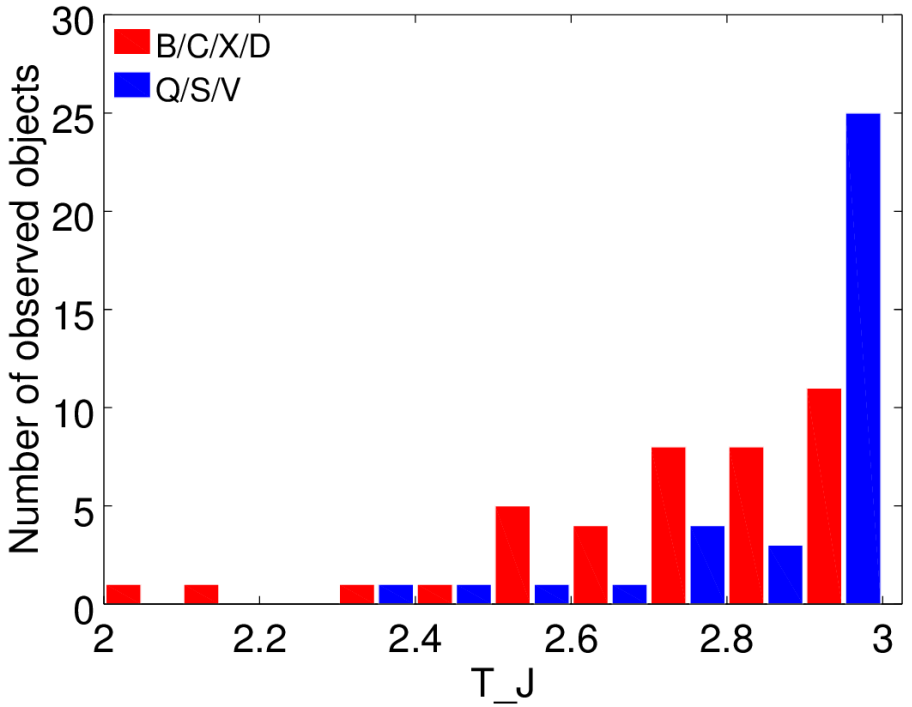

2007 VA85 - 333P/LINEAR

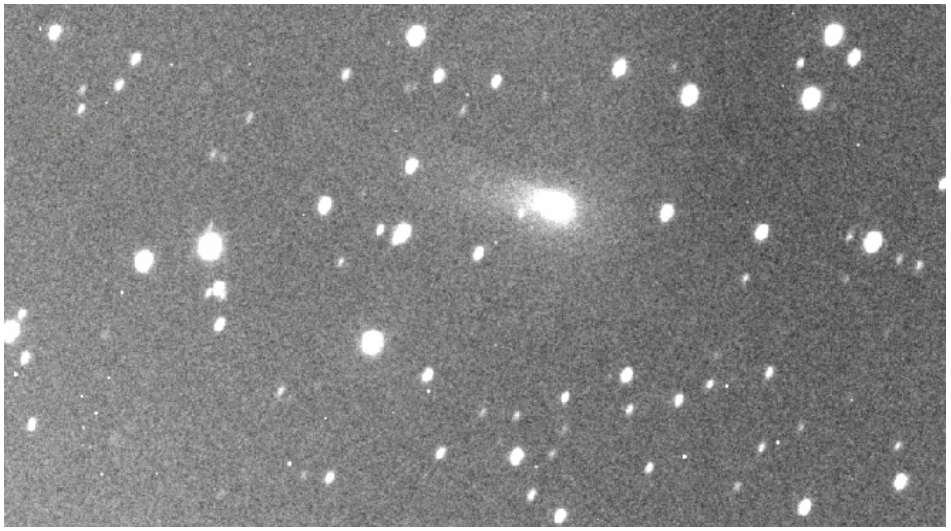

2007 VA85 observed at T1m/ Pic du Midi on 2016-04-06

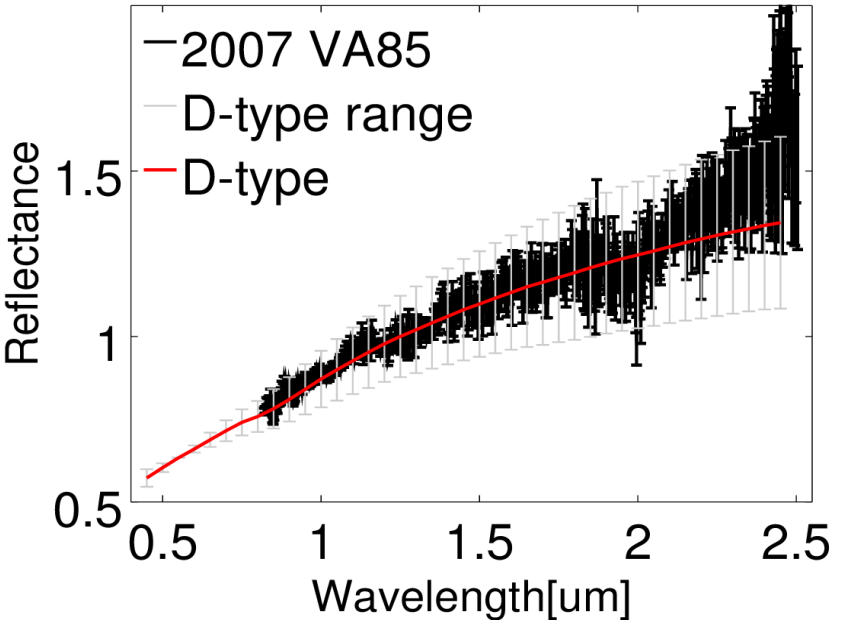

- Discovered as asteroid 2007 VA85
- Cometary activity detected on early 2016
- TJ = 0.418, retrograde orbit
- D-type spectrum

Paper in preparation

(52381) 1993 HA

- ✔ 1993 HA is a very favourable target for a space mission based on its dynamical properties (low-ΔV: 5.302), with a mission a mission duration of 3.6 years.
- ✔ our visible and near-infrared data show that this object is a rare **D-type NEA**
- ✔ size of 0.337 +0.097/−0.078 km based on an albedo of 0.140 −0.077/+0.110 (ExploreNEOs survey, Trilling et al. 2010), thus less probable, a T- or X-type classification
- ✔ we measured a synodic rotation period of 4.107±0.002 h. An elongated shape, with a derived lower limit for the axis ratio a/b=1.71.

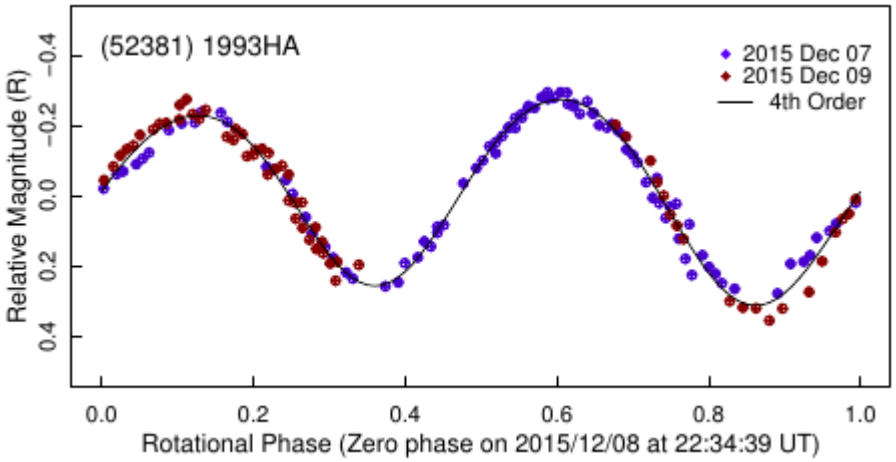

Composite lightcurve of 1993 HA, folded with a synodic period of 4.107 h. The average error is of ~0.015 mag.

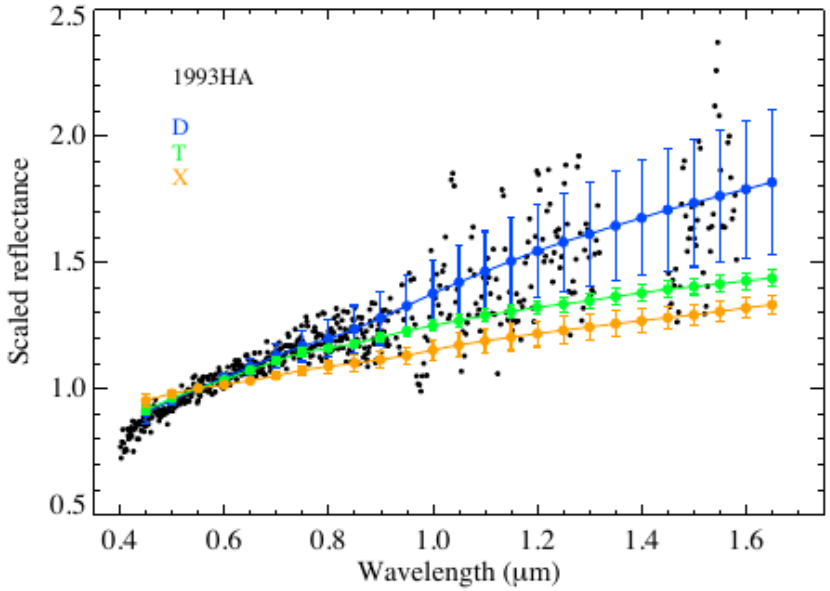

Combined visible and near-infrared spectrum of 1993 HA (EFOSC2 + SOfI at ESO-NTT). The average spectra of D-, T- and X- type are shown for comparison.

Perna et. al; A&A, 2017

M4AST - Modeling for Asteroids Spectra

A tool dedicated to asteroid spectra;

- It consist of:
  - A set of applications for analyzing asteroid spectra;
  - Spectral database (2,700 spectra of asteroids);
  - Planning the observations tool;
- Is fully available via a web interface.
- www.m4ast.imcce.fr

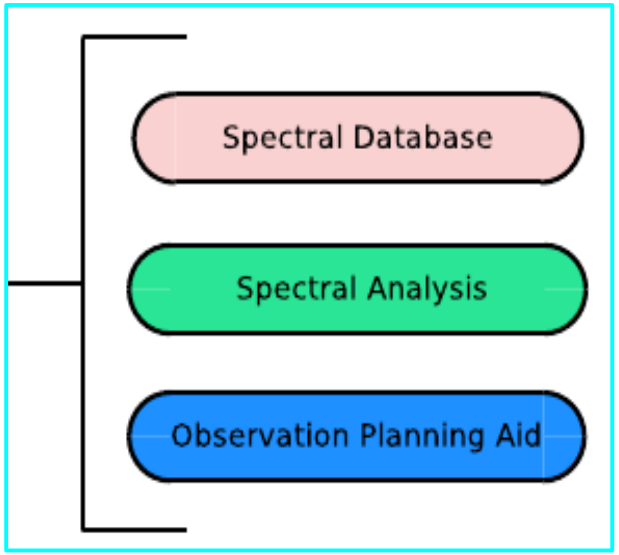

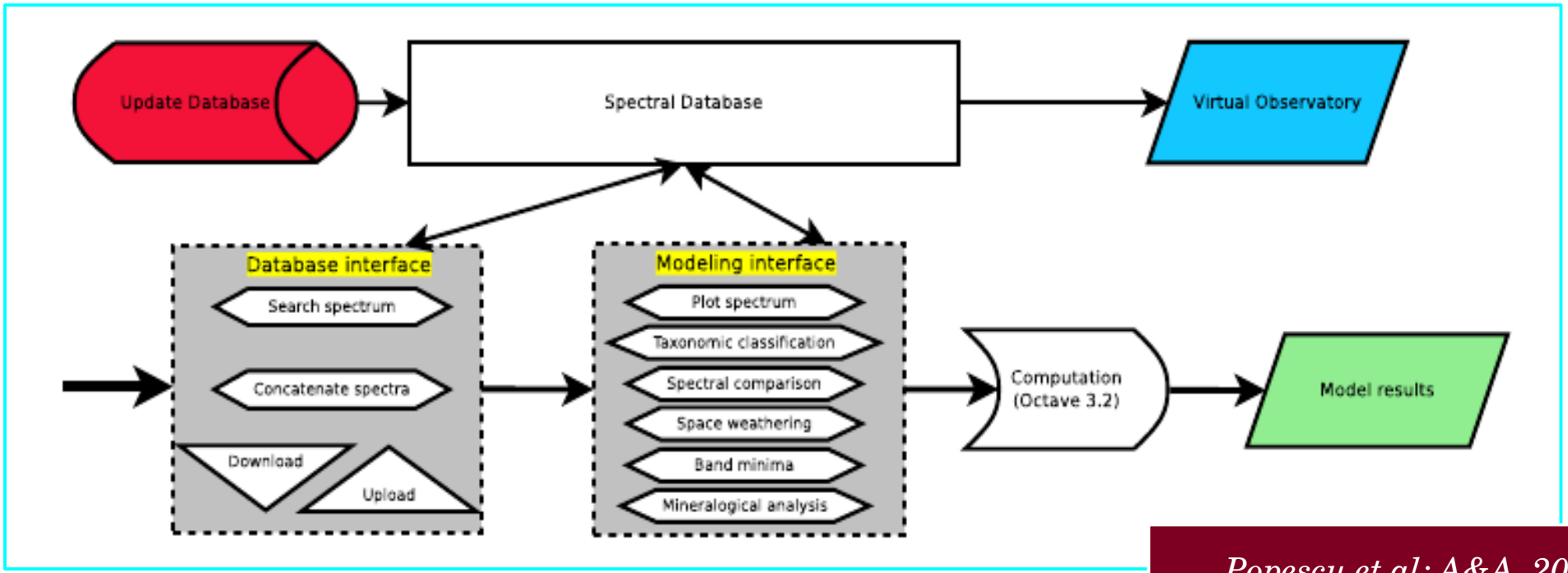

Popescu et.al; A&A, 2012

The global picture of asteroids population

- Spectral data available for ~3,000 objects. VNIR spectral data available for ~2,000 objects;
- - DeMeo & Carry 2014 used SDSS and WISE data to create a global picture over 100,000 asteroids;
- - SDSS and WISE data allows to group the minor planets population in a few major classes, without reflecting the diversity revealed by the small number of spectra.
- - Even this sparse data shows a compositional mixing between different orbital groups, which points to a turbulent history of the solar system (DeMeo & Carry 2014).

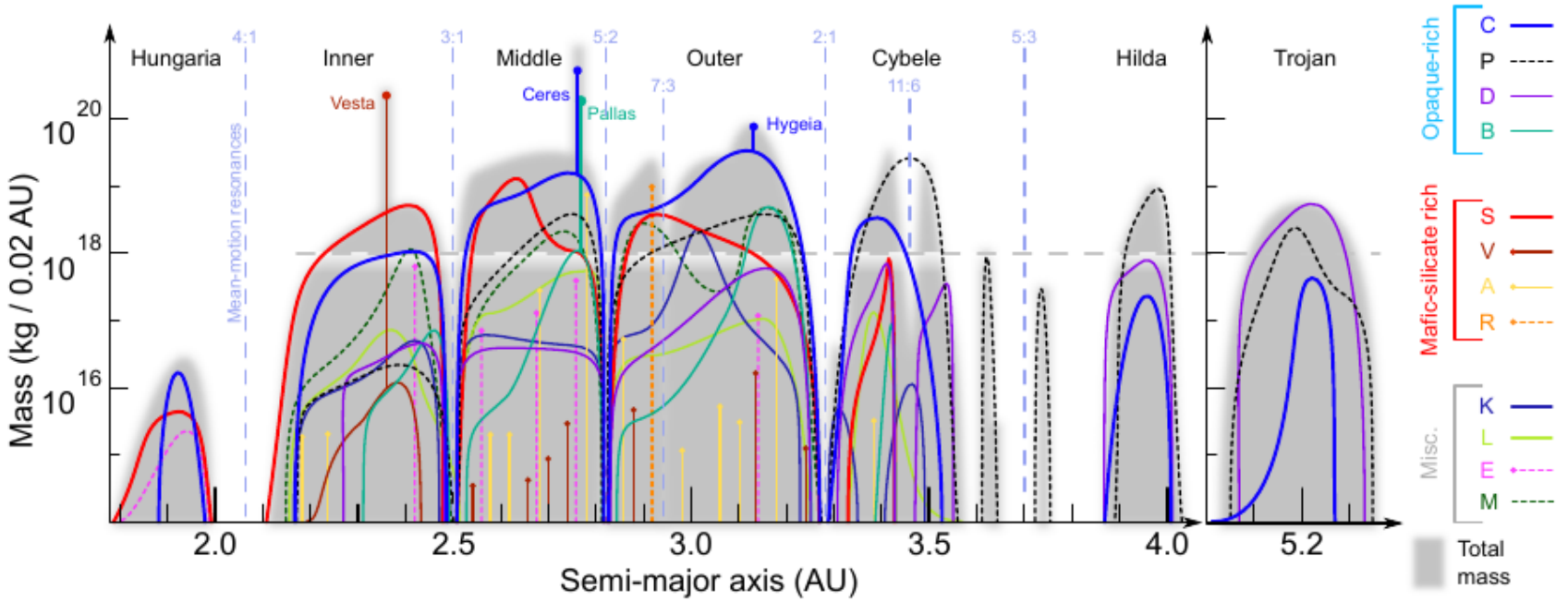

The compositional mass distribution throughout the asteroid belt based on visible colors and surface brightness from WISE and SDSS survey. Source: DeMeo & Carry 2014.

Sampling the spectra with Y, J, H, Ks filters

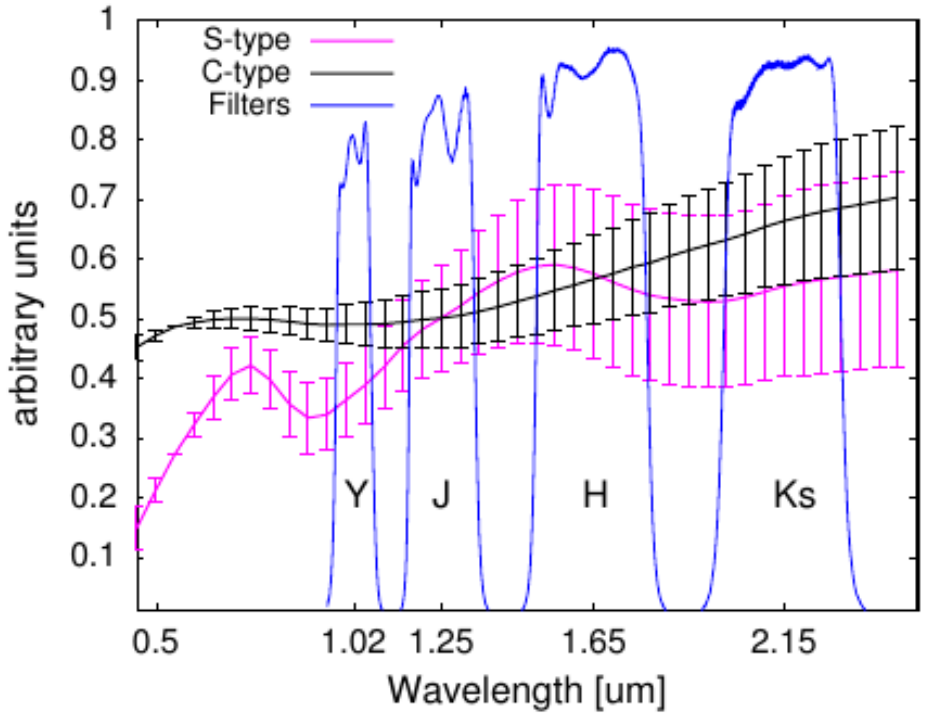

The wavelength position of Y, J, H, and Ks filters compared with the standard S and C taxonomic types from DeMeo et al. (2009).

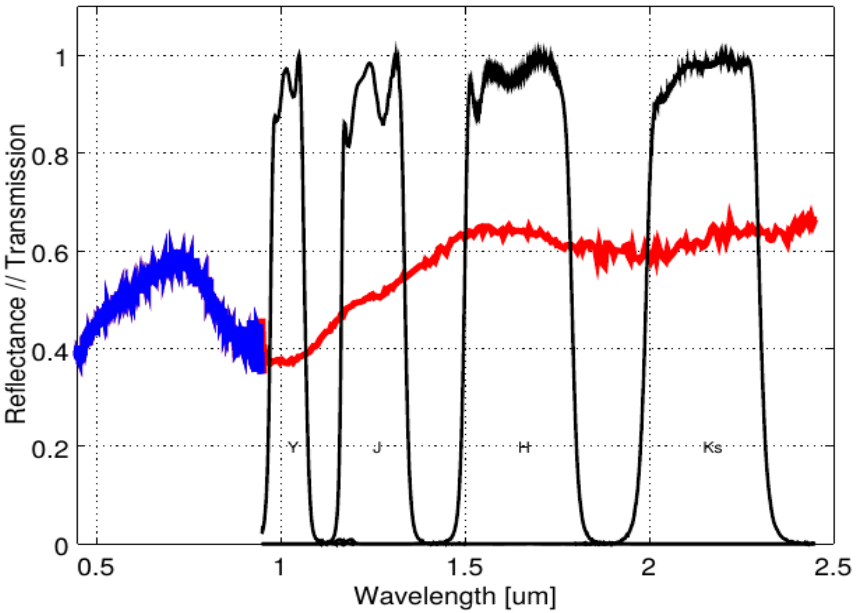

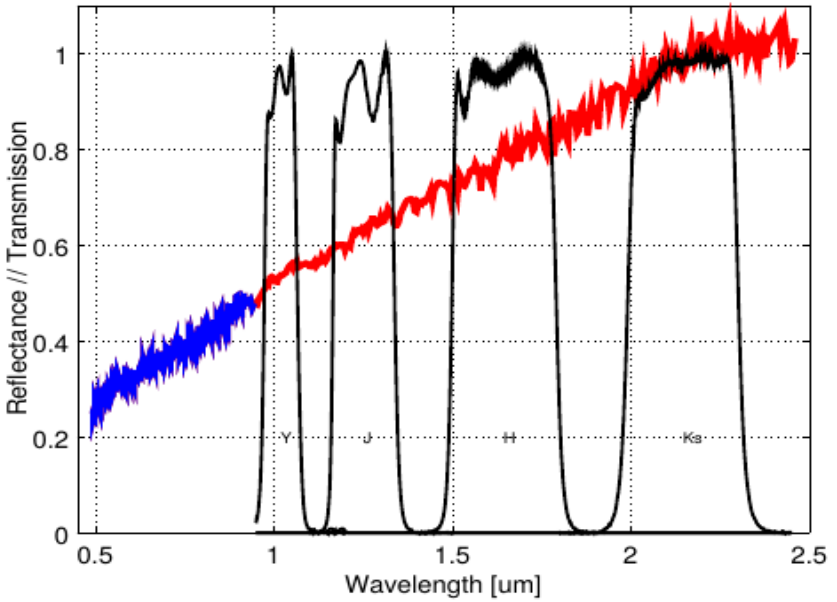

Insights into asteroid surface composition may be obtained even using the broadband filters Y, J, H, Ks.

Spectra of a Q-type asteroid - (5143) Heracles (upper right), and of a M-type asteroid -(1280) Baillauda (lower left) are shown.

New large set of NIR data! from VISTA

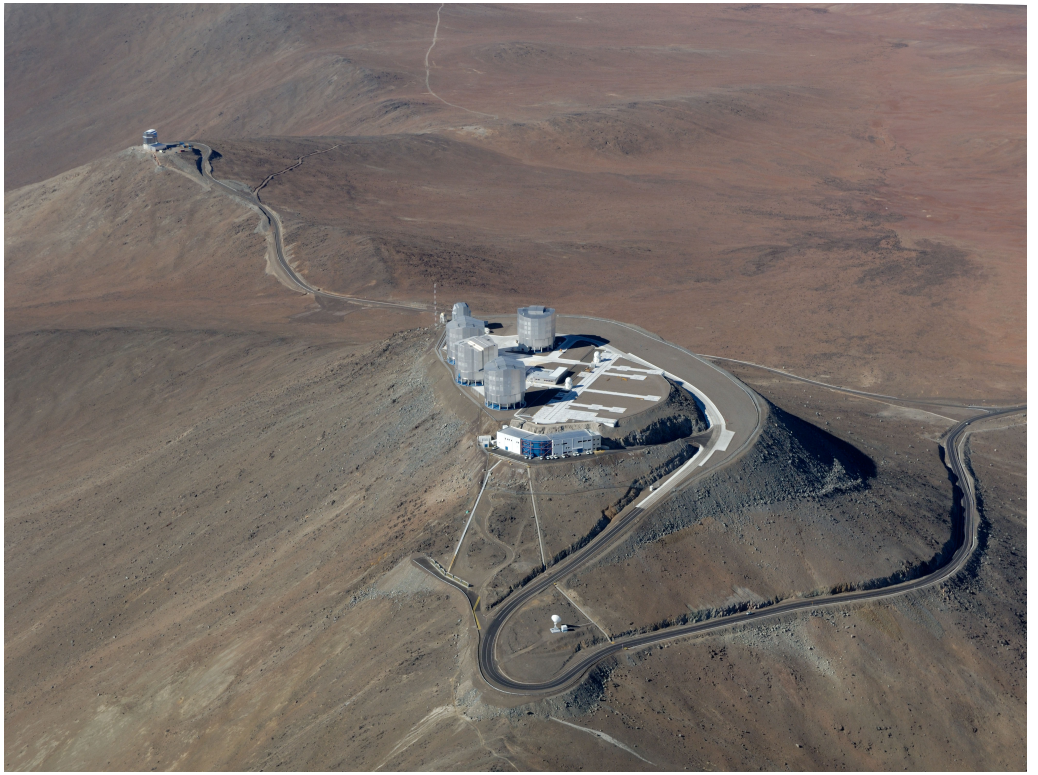

VISTA telescope on ESO Paranal. Source: http://www.eso.org/sci/facilities/paranal/instruments/vircam.html, http://www.vista.ac.uk/Images/site/hires/VISTAandParanal.jpg

- VISTA (Visible and Infrared Survey Telescope for Astronomy) is a 4-m class dedicated to wide field survey telescope for the southern hemisphere;
- Near infrared camera VIRCAM (VISTA InfraRed CAMera)
- VHS: VISTA Hemisphere Survey : The VHS will image the entire southern hemisphere of the sky; 4 magnitudes deeper than the earlier 2MASS and DENIS surveys.

VISTA – VHS sky coverage

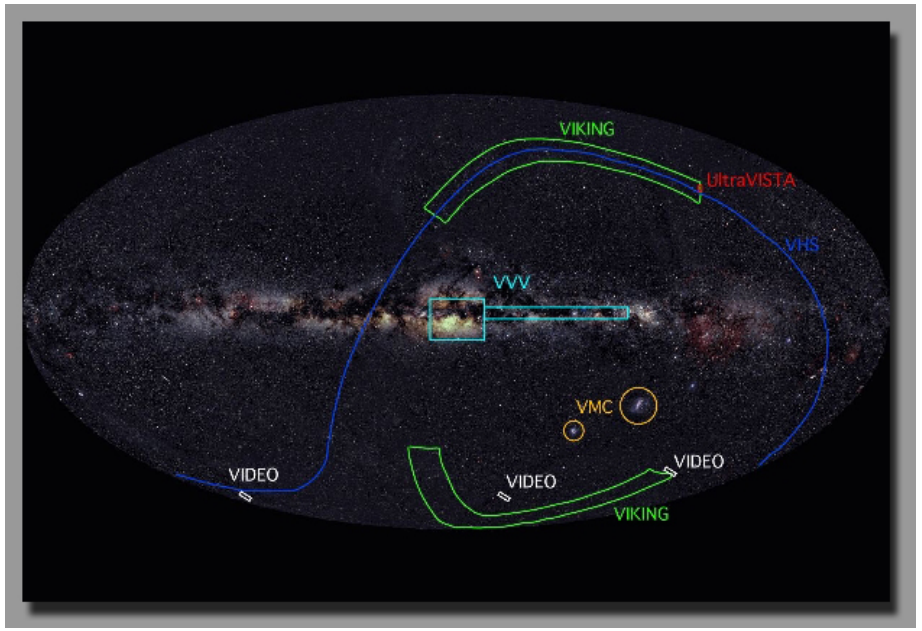

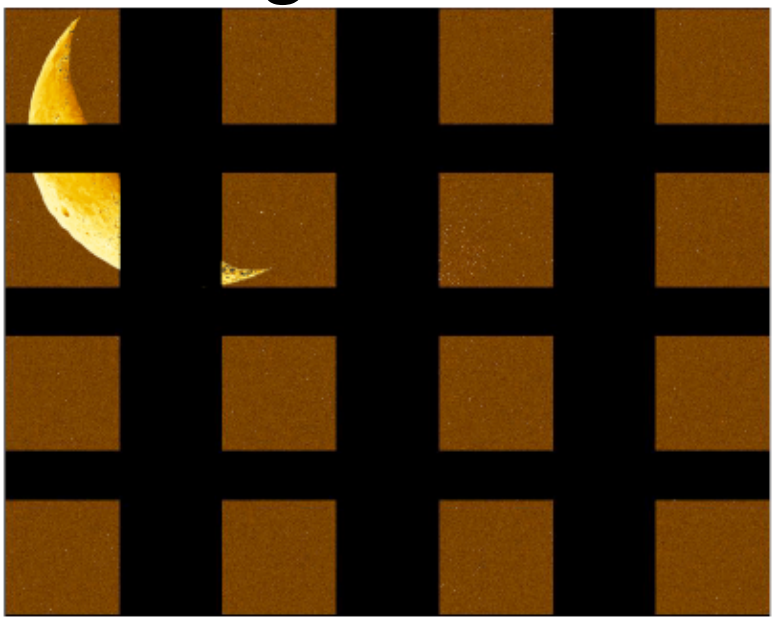

Camera FOV: 1.3^{O} x 1.02^{O}

VHS (upper right fig.) is a panoramic wide field Infra-Red sky survey, which will result in coverage of the whole southern celestial hemisphere (~19,000 deg2)

- VHS ATLAS (5000 deg2): exposures in Y, J, H, and Ks
- VHS Dark Energy Survey (4500 deg2):exposures in J, H, and Ks
- VHS GPS (8200 deg2): J and Ks

Each VISTA tile stack (lower left fig.) requires 6 sparse filled pawprints (upper right fig.)

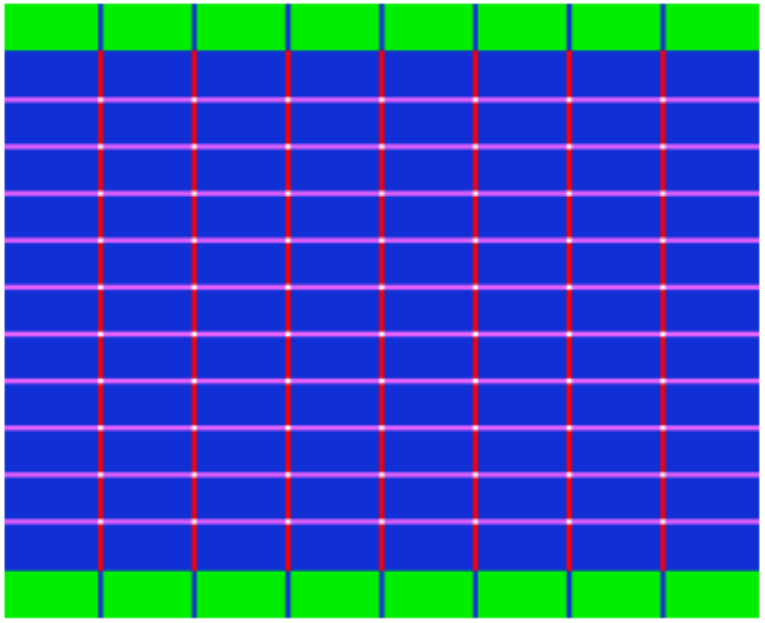

Exposure map of VISTA tile (1 -green, 2-blue, 3-pink)

Algorithm

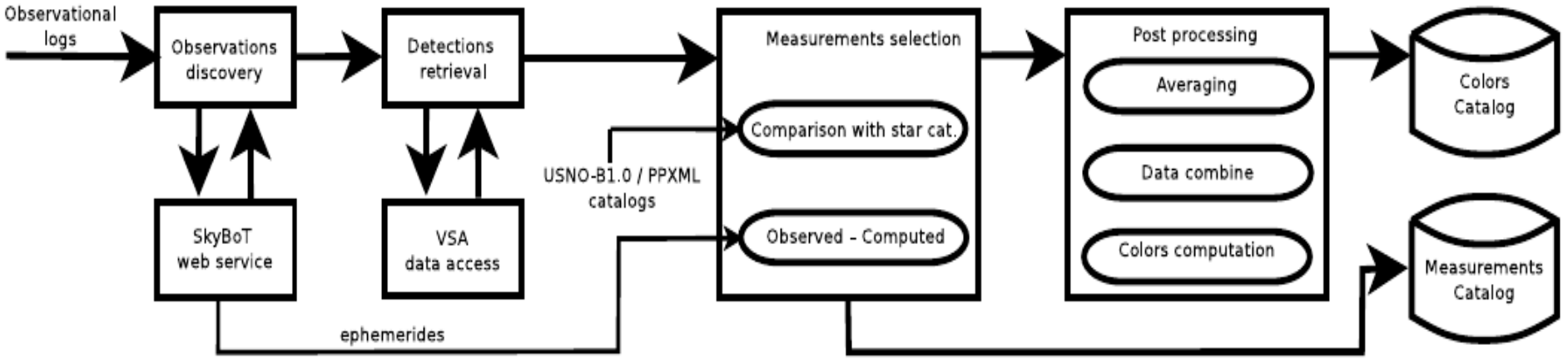

Flowchart of MOVIS pipeline

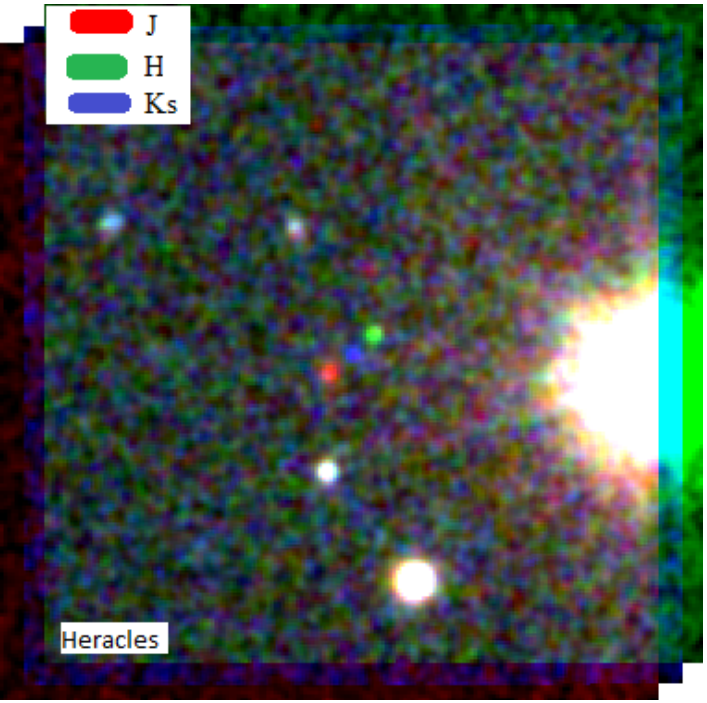

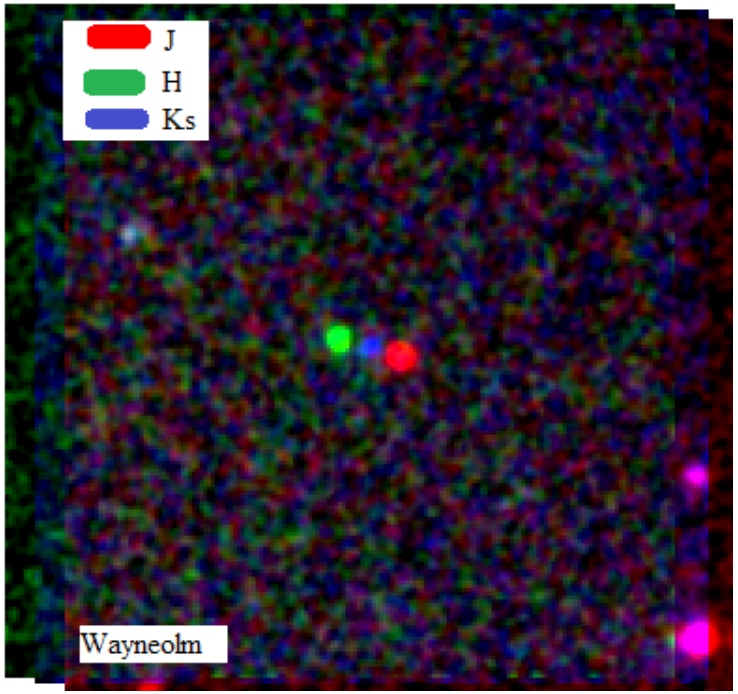

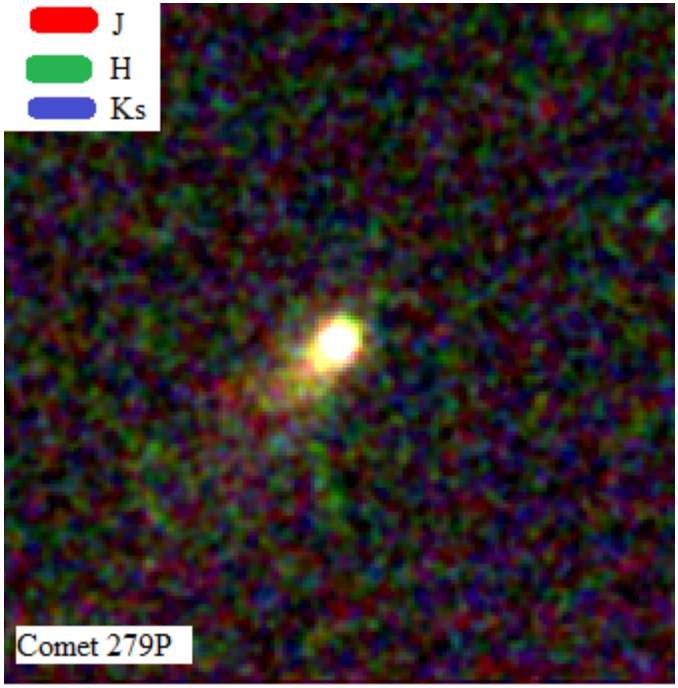

False color image obtained by combining the stack frames observed with J, Ks and H filter

Discovering the observations of minor planets

Predictions

- Accurate timing is crucial for Solar System objects (Sso);
- RA, DEC, MJD are the input data for Simple Cone Search (SCS) web-service provided by SkyBoT (Berthier, 2006);
- The SkyBoT cone-search method allows to retrieve all the known solar system objects located in a field of view;
- 300 queries/hour & monitoring routine for reliability;
- 68 237 objects found, 62 340 objects with uncertainty lower than 10 arcsec.

Detections

- The VISTA Data Flow System - VDFS (Emerson et al. 2004) is the pipeline that accomplish the end-to-end requirements of the VISTA survey
- All the detections (a detection is referring to a single object extracted from a single image in a single filter) found in VISTA survey images are stored in the vhsDetection table
- The cross-matching imply a square box search centered at the predicted position in vhsDetection table. The side of the box is 6σ, but no less than 2 arcsec
- 332 111 detections corresponding to 47 666 objects

Popescu et.al; A&A, 2016

Miss-identifications and errors

- Limiting V magnitude: 21. Magnitude error distributions confirms the cutting V-magnitudes and validations criteria
- Aperture photometry: 1 arcsec aperture radius.
- Analysis of individual objects should be done after investigating the images, to avoid miss-interpretations

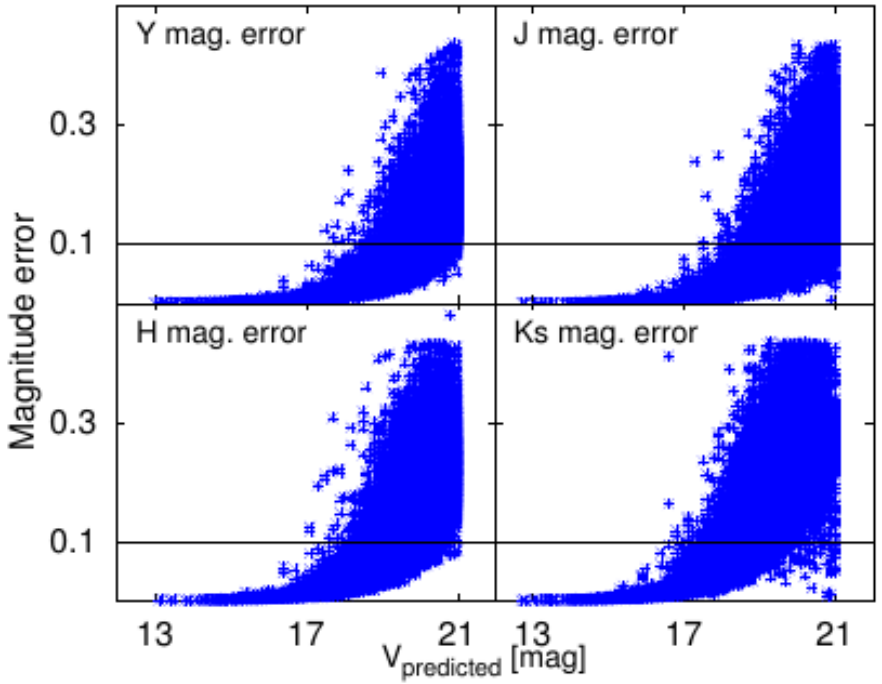

The magnitude error distribution for all valid detections

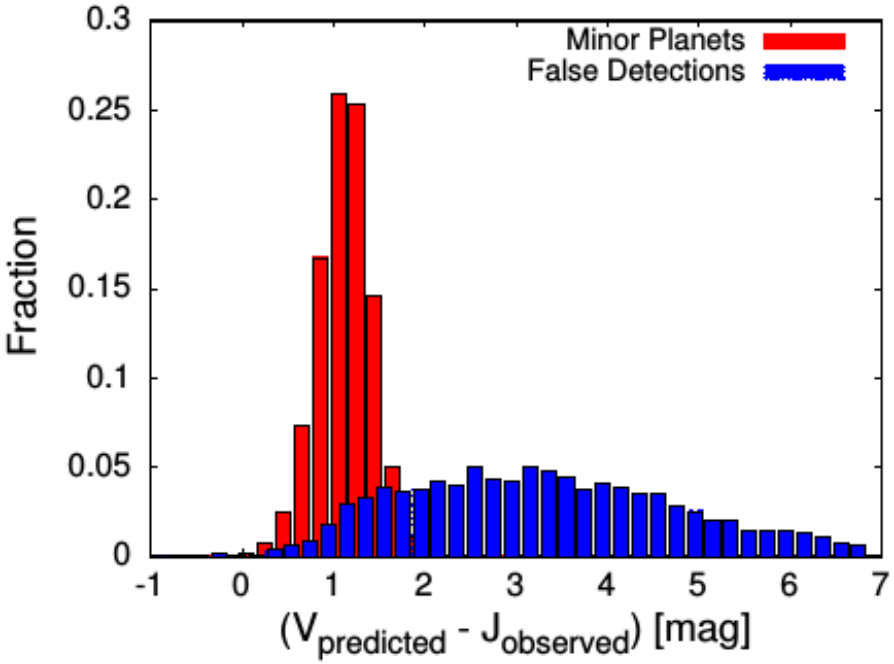

The difference between predicted V magnitudes and observed J magnitudes .

Popescu et.al; A&A, 2016

Post-processing of the data

- **Post-processing:**
  - a) Average measurements obtained with the same filter in an interval less than 15 minutes;
  - b) Select magnitudes obtained with different filters such that the interval between observations to be minimum;
  - c) Obtain colors by combining the closest in time observations from two different filters;
  - d) Combine colors obtained at different epochs.

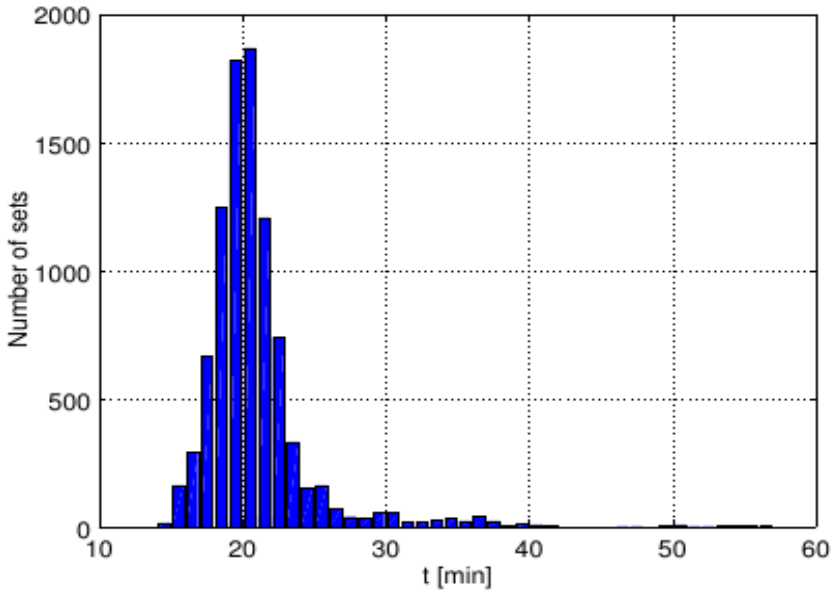

The distribution of the time intervals in which the observations sets containing all 4 filters were performed.

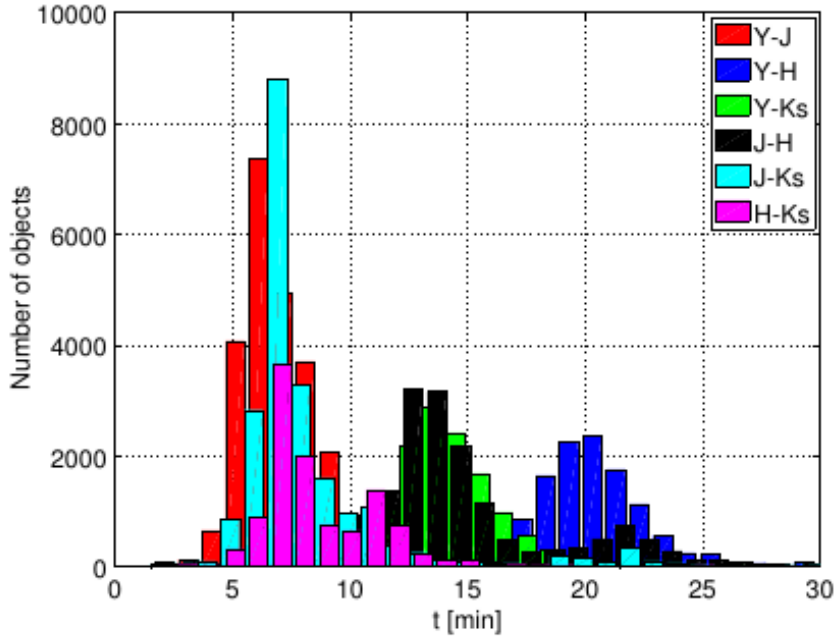

The time interval between the two observations used to compute the colors

MOVIS Catalogs

- The results of the recovering pipeline are split catalogs:
  - ✔ the detections catalog (MOVIS-D);
  - ✔ the magnitudes catalog (MOVIS-M);
  - ✔ the colors catalog (MOVIS-C);
- Data was uploaded to CDS-Strasbourg, all three catalogs are accessible via VO services.

A total of 39 947 objects, including:

- - 52 NEAs,
- - 325 Mars Crossers,
- - 515 Hungaria asteroids,
- - 38 428 main-belt asteroids,
- - 146 Cybele asteroids,
- - 147 Hilda asteroids,
- - 270 Trojans,
- - 13 comets,
- - 12 Kuiper Belt objects

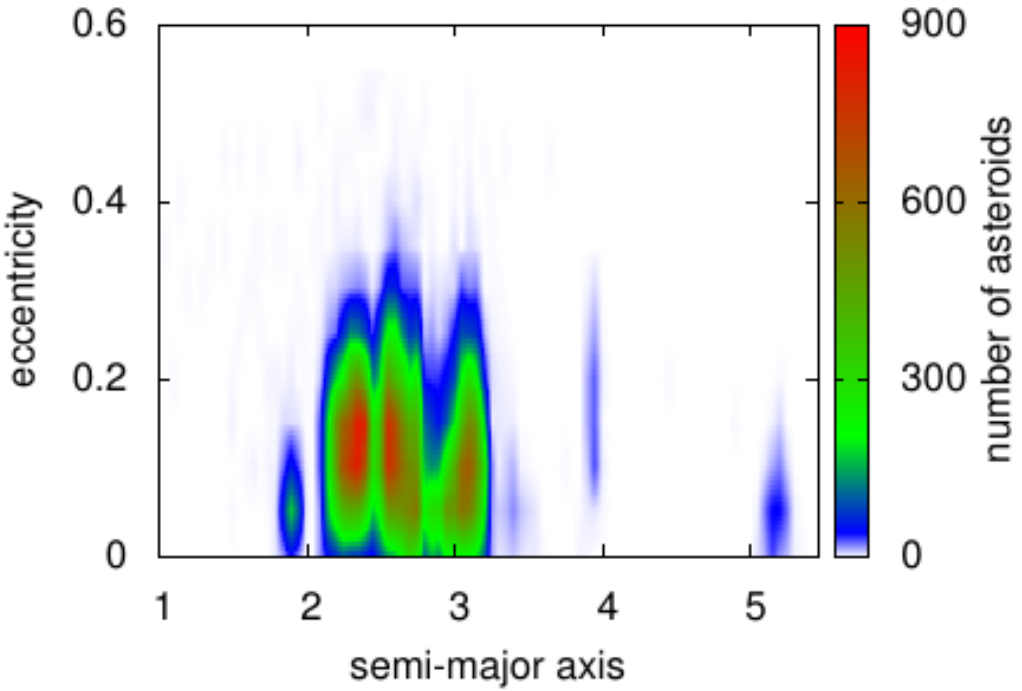

Distribution of the observed objects on semi-major axis and eccentricity.

Compute the equivalent of taxonomic types

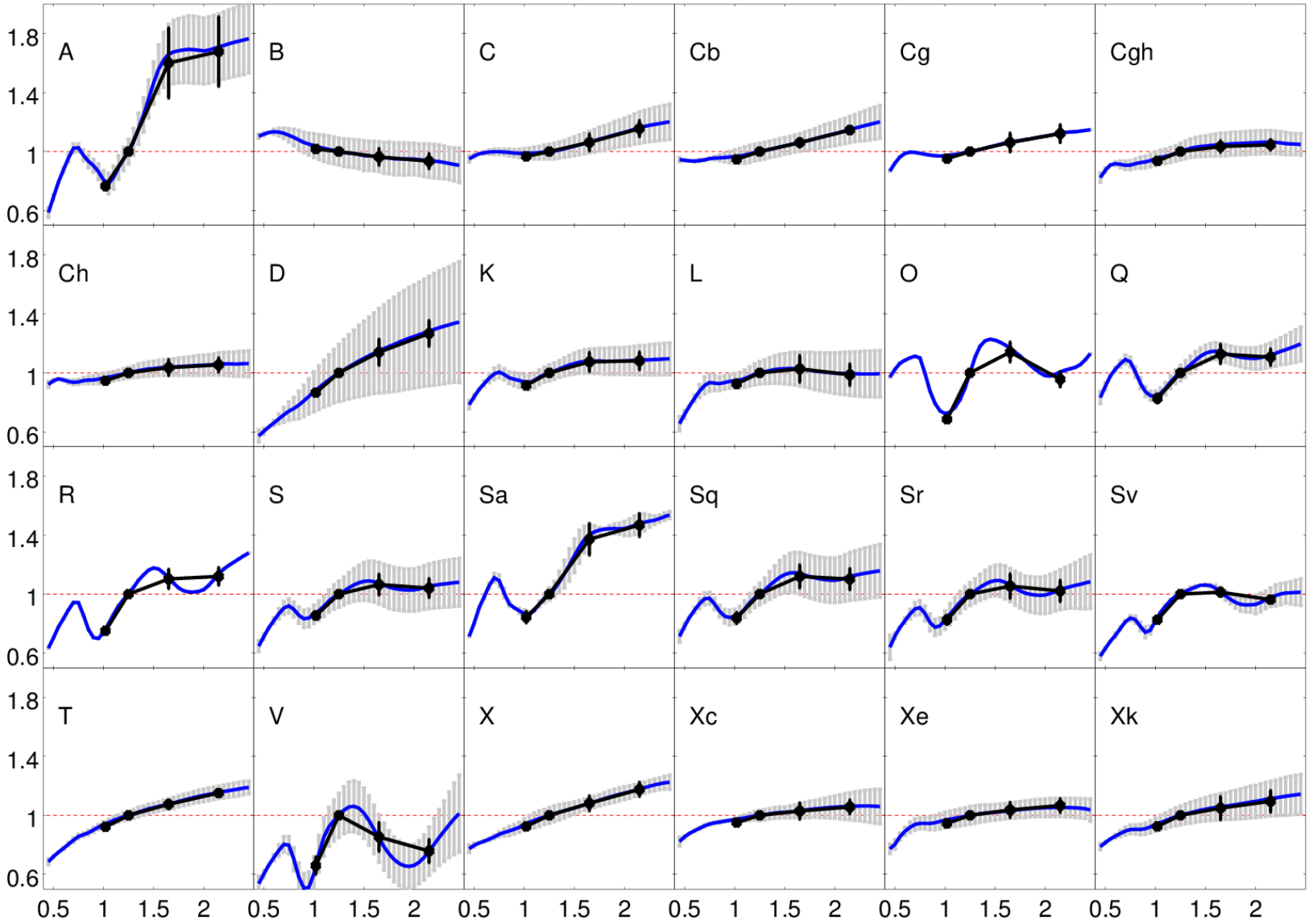

Color-color plots and spectral classes

- Studies focused on determining the NIR colors of individual asteroids of interest, or families, or studying specifying taxonomic types (Leake 1978, Veeder 1982,1983, Hahn&Lagerkvist 1988, Gaffey 1989, Hainaut 2002)
- Sykes 2000, mapping of A,S, C, D type in the J-H vs H-Ks plot. High SNR data is consistent with the reported classes
- Greater infill across the different taxonomic classes in 2MASS

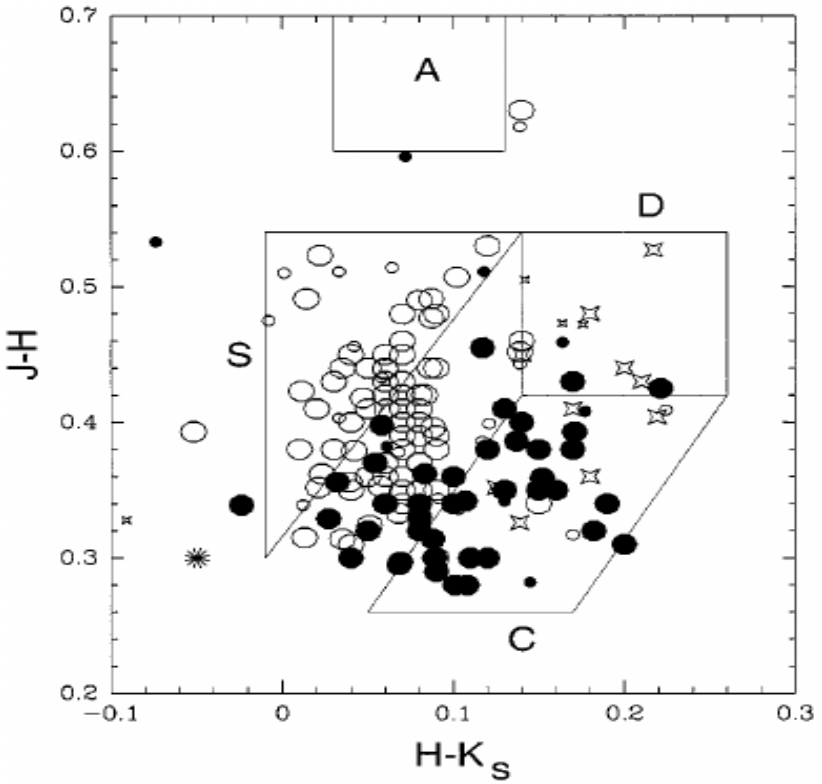

2MASS data (Sykes, 2000) - SNR>30. Open circles -> S type, filled circles -> C-type, and stars -> D-type.

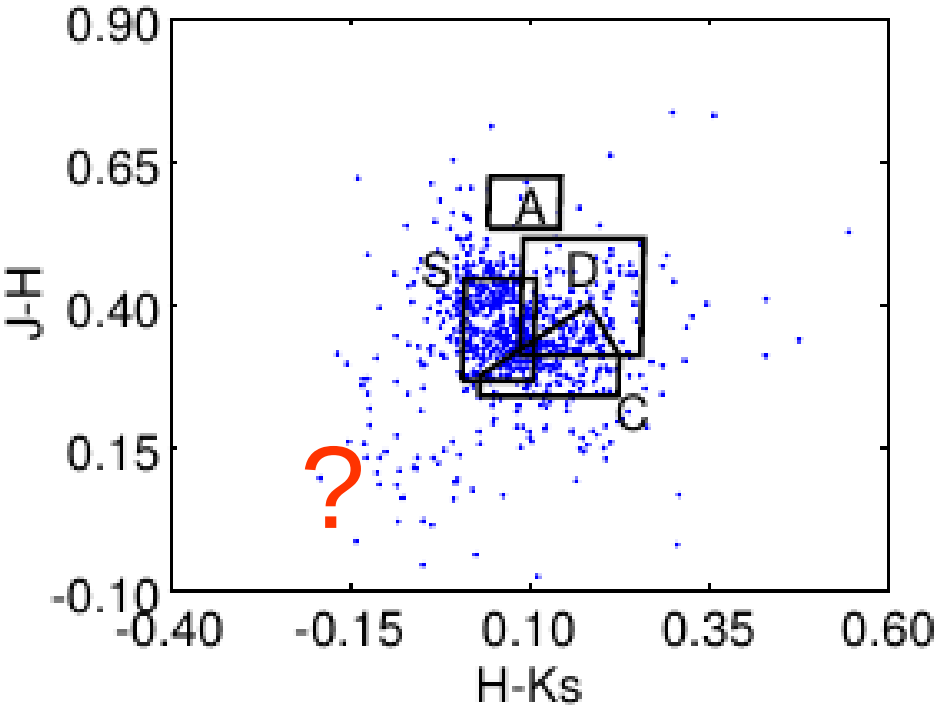

VHS-VISTA, SNR>30(1500 points considered). The regions found by Sykes et al. (2000) are shown with black lines.

Methods for mapping color-color plots

- Identify groups of minor planets that have similar surface composition match them with the taxonomic types.
- Map the colors of asteroids with known spectral behavior form SMASSI (Xu et al. 1995), SMASSII (Bus & Binzel 2002b,b), and S3OS2 (Lazzaro et al. 2004).
- Compare the distribution of MOVIS-C data in color-color space with the position of colors computed for the template spectra defined by DeMeo et al. (2009).
- We computed the equivalent of the spectral templates into the colors domain by taking into account the response curve of the filters and the solar colors.

C-complex: B, C, Cb, Cg, Cgh, and Ch; S-complex: Q, S, Sq, Sr, and Sv; X-complex includes X, Xc, Xe, and Xk; A class includes A and Sa types.`

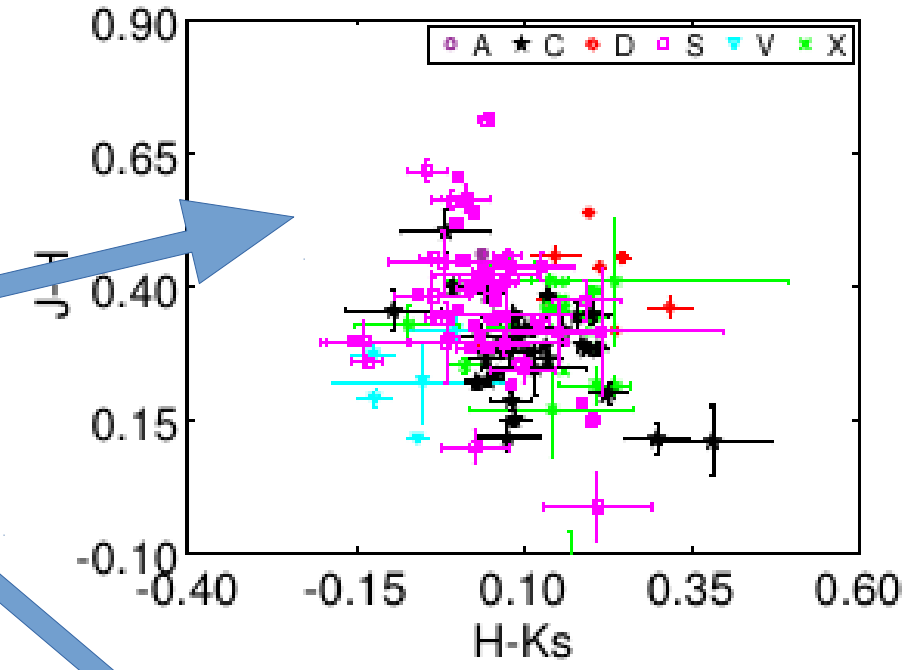

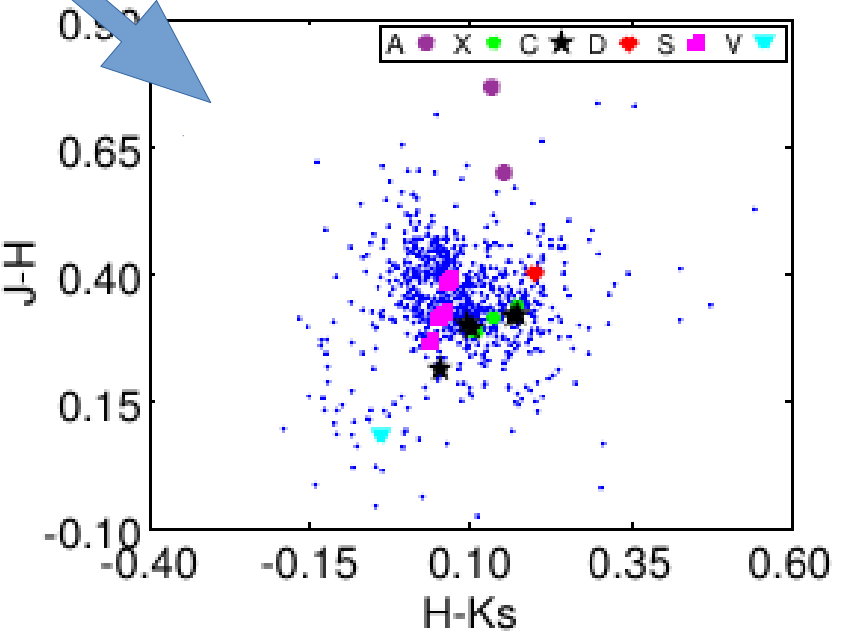

(Y-J) vs (J-Ks) plot

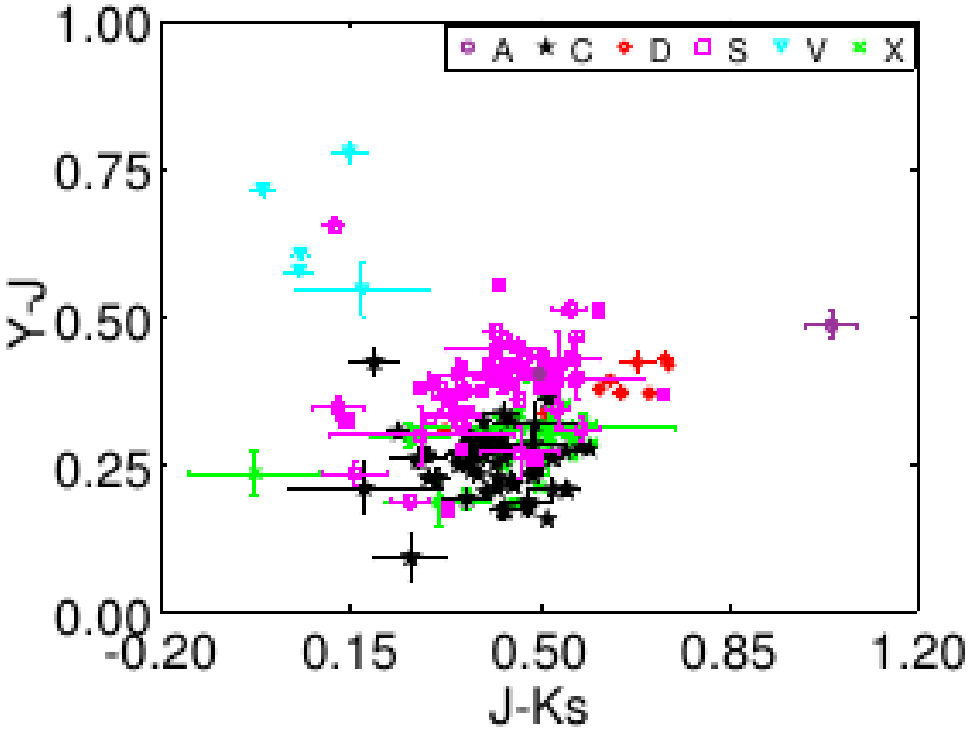

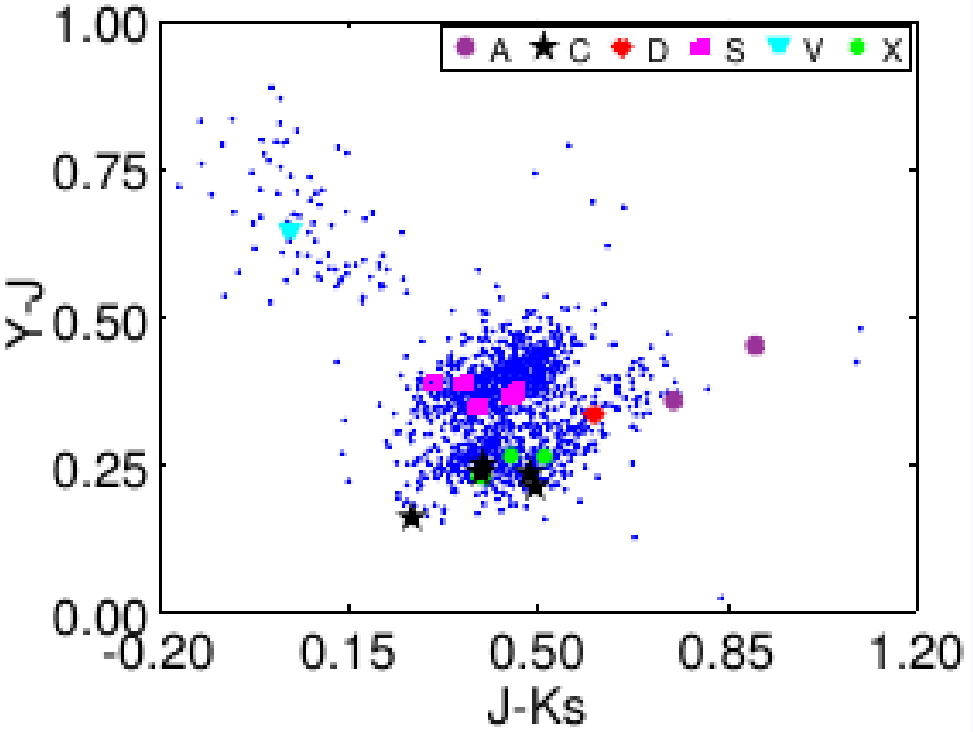

(Left) The colors of asteroids with visible spectra, having an assigned taxonomic type. **(Right)** The colors computed for the template spectra of the taxonomic classes from DeMeo et al. (2009) compared with the MOVIS-C data with color errors less than 0.033. *C-complex: B, C, Cb, Cg, Cgh, and Ch; S-complex: Q, S, Sq, Sr, and Sv; X-complex: X, Xc, Xe, and Xk sub-classes and is denoted as X; A class: A and Sa.*

- The plot shows the gap between the S-complex and the C/X-complex.
- The colors of taxonomic templates are in the regions with high density number of objects.
- The data corresponding to the S-complex template spectra appear as a compact group.
- The C-complex, is divided in three groups.
- A borderline between S and C can be drawn: $(Y-J) = 0.412^{\pm 0.046} \cdot (J-Ks) + 0.155^{\pm 0.016}$

Taxonomic classification based on near-infrared colors

➢ **Method I.** map the Y-J versus J-Ks plot; objects with accurate photometry can be easily classified.

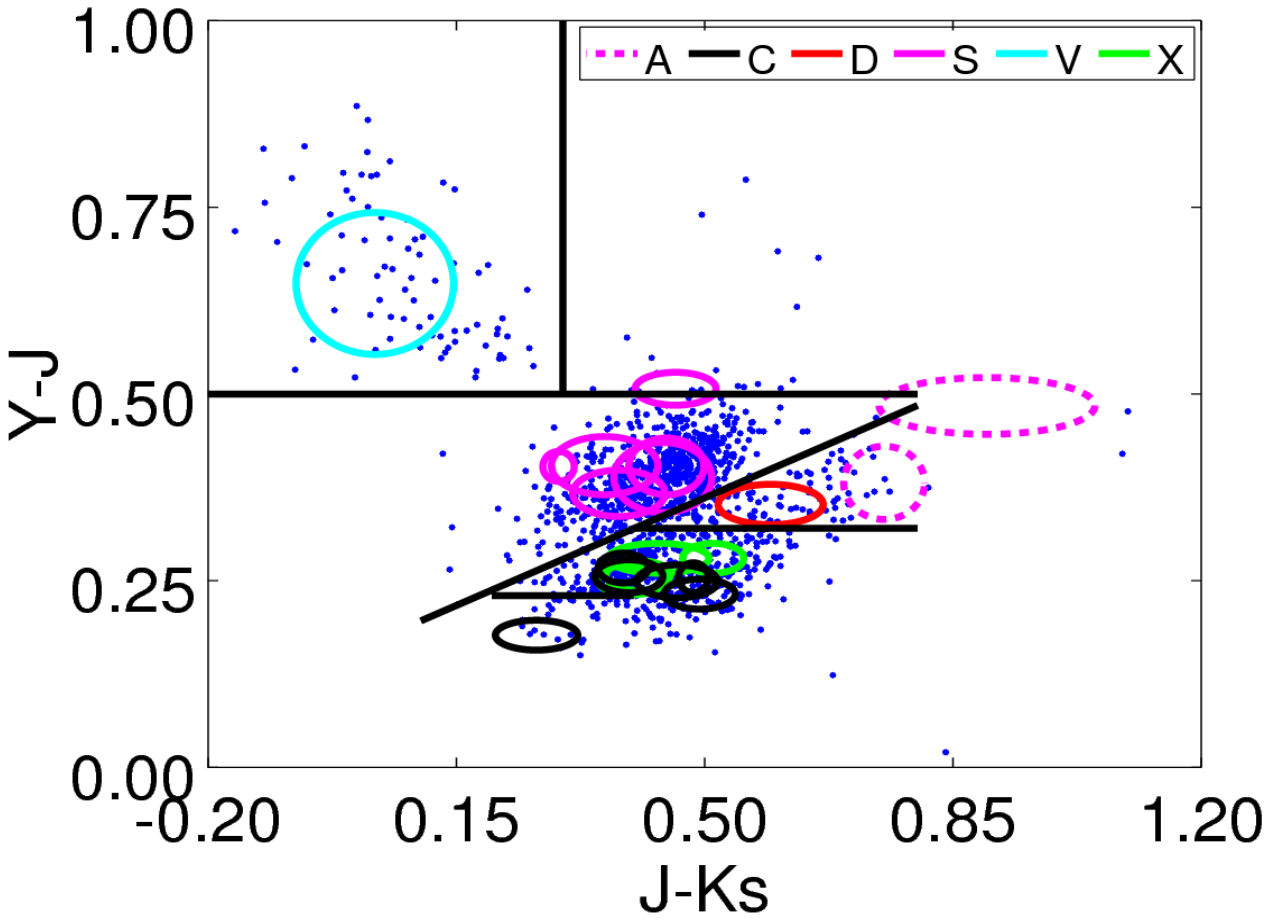

The (Y-J) vs (J-Ks) plot of objects with color errors less than 0.033. Overlapped are the taxonomic types from Bus-DeMeo taxonomy with the corresponding standard deviations.

(Y-J) vs (J-Ks) plot: data with color error<0.1

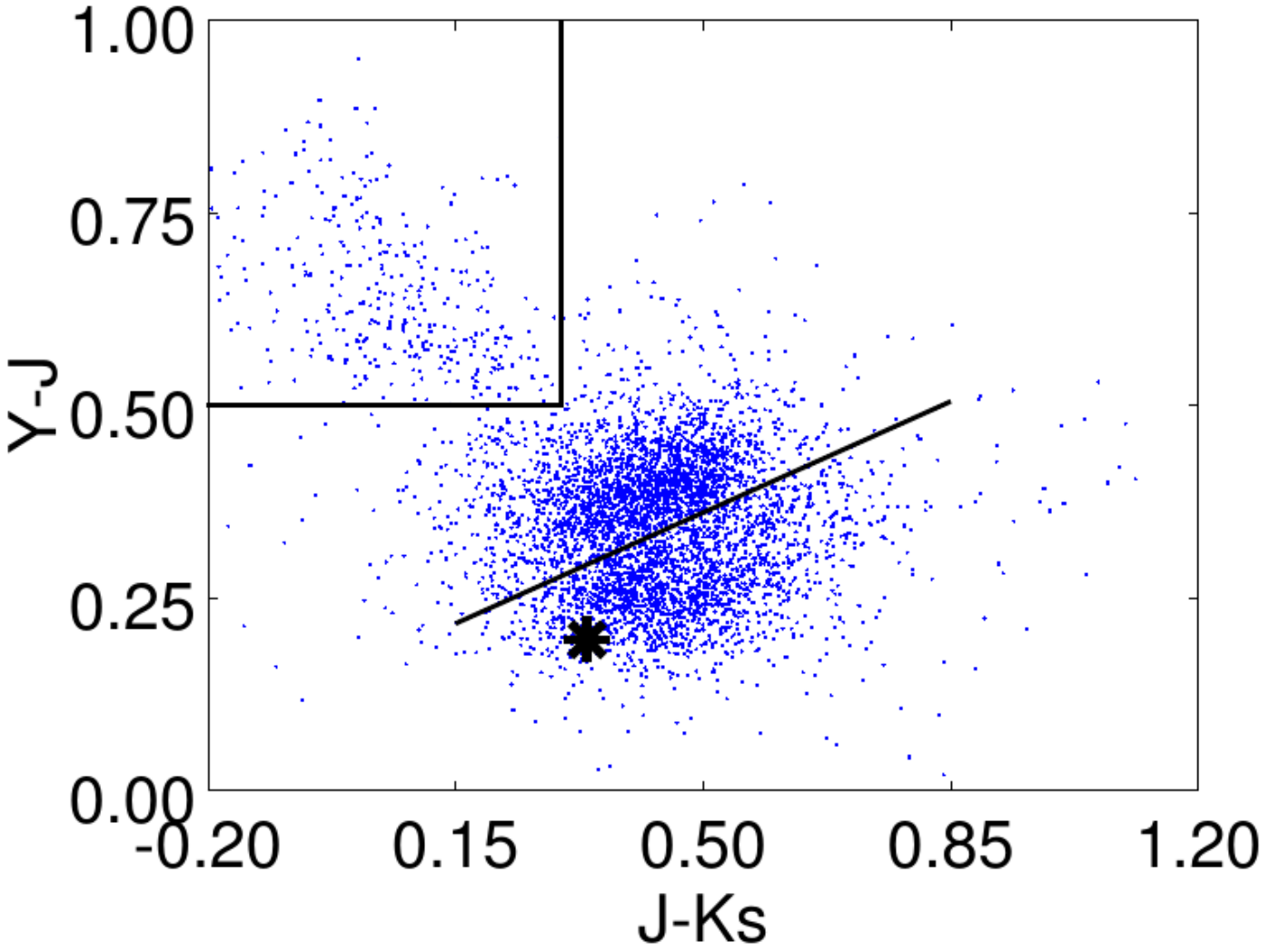

The (Y-J) vs (J-Ks) plot of objects with color errors less than 0.10 is consistent with the distributions discussed above. The clusters corresponding to S- and C/X complexes are identifiable even for large errors.

Taxonomic classification based on near-infrared colors

Method II.

- Probabilistic approach (e.g. Carvano et al. (2010): 1) for each object calculate the probabilities for its available colours to be compatible with the 24 classes; 2) the probability that a set of colours corresponds to a taxonomic class is the product of the probabilities of each colour;

- Machine-learning methods available with scikit-learn module for Python: Extreme Gradient Boosting (XGB), Random Forests(RF) with different parameters, and Nearest Neighbour (kNN)

Table 2: Comparison between different classification algorithms based on "leave-one-out". Acc_{YJHKs} is the accuracy obtained when running the algorithm with all three colors, and Acc_{YJKs} was obtained for two colors.

Algorithm	$Acc_{YJHKs}[\%]$	$Acc_{YJKs}[\%]$
XGB	87.8	84.6
RF leaf 1	86.2	85.4
RF leaf 2	86.2	85.6
RF leaf 3	85.6	85.4
RF leaf 4	85.4	84.6
kNN 3	87.0	84.6
kNN 5	87.0	85.9
Prob	81.8	81.8

Popescu et.al; paper in preparation

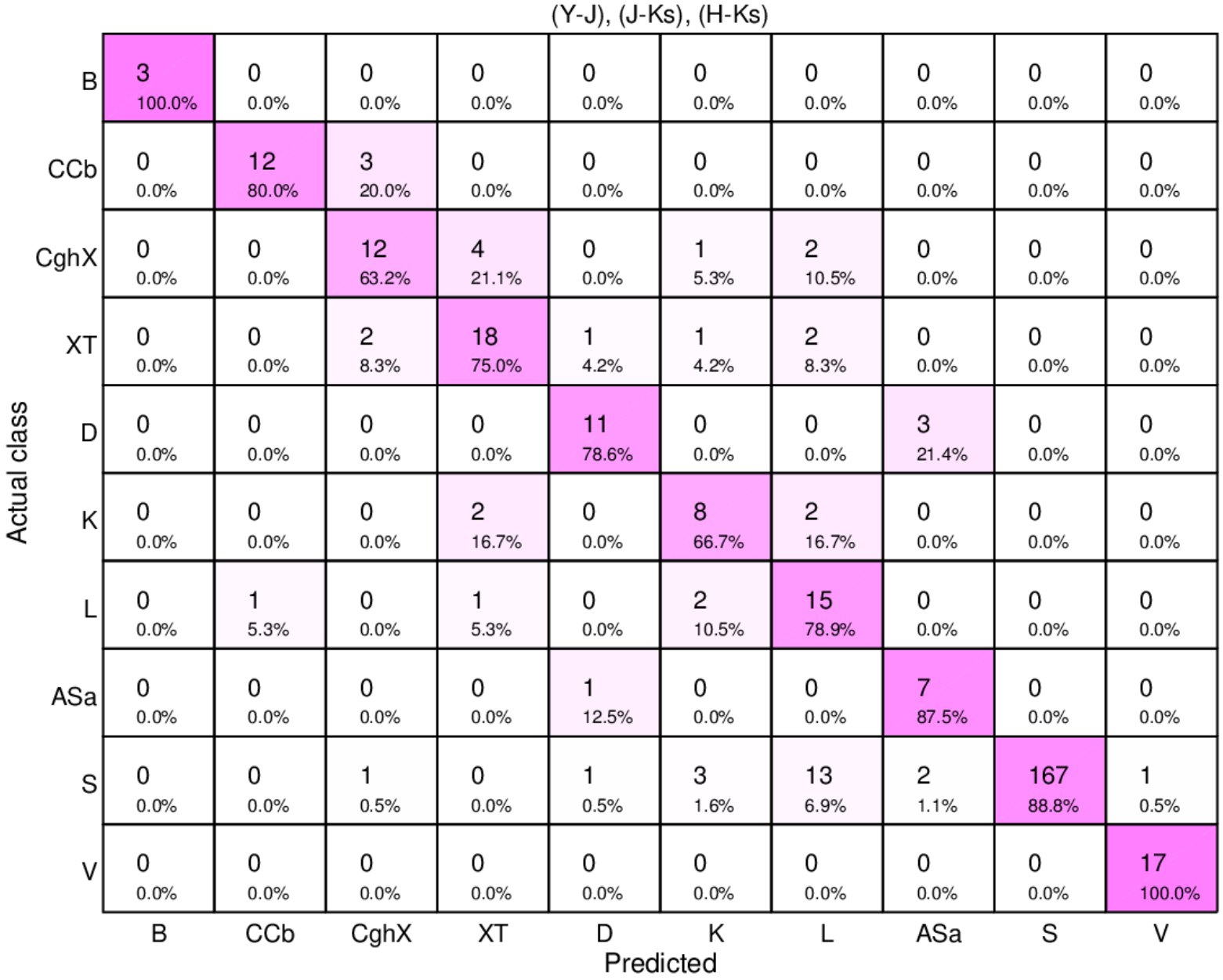

The confusion matrix of kNN3 algorithm obtained after "leave-one-out" cross-validation. The predicted class by the algorithm based on their computed colors are shown versus the spectral classification (labeled actual class) for the 371 samples of the reference set.

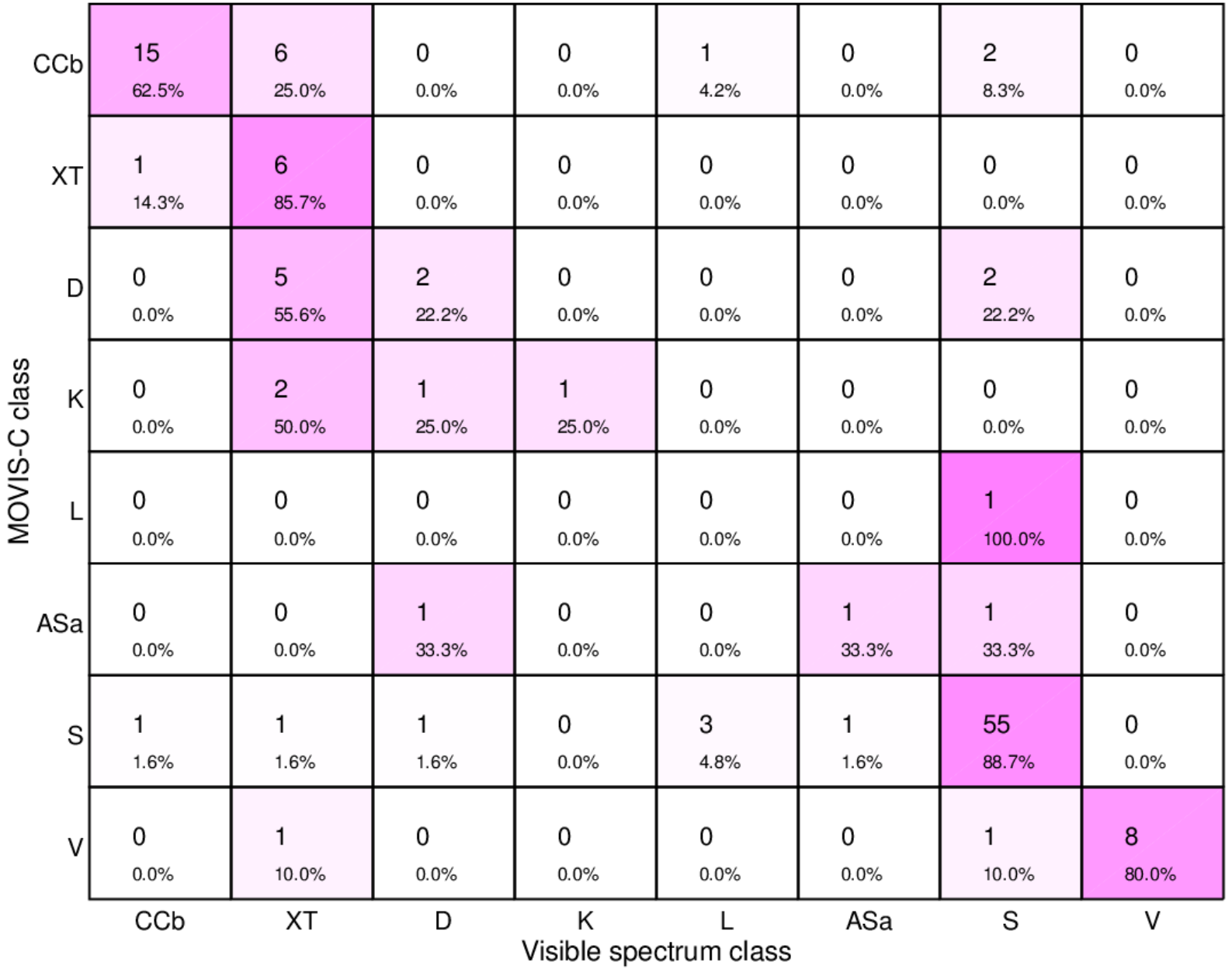
MOVIS-C class
CCb
XT
D
K
L
ASa
S
V
15 62.5%
6 25.0%
0 0.0%
0 0.0%
1 4.2%
0 0.0%
2 8.3%
0 0.0%
1 14.3%
6 85.7%
0 0.0%
0 0.0%
0 0.0%
0 0.0%
0 0.0%
0 0.0%
0 0.0%
5 55.6%
2 22.2%
0 0.0%
0 0.0%
0 0.0%
2 22.2%
0 0.0%
0 0.0%
2 50.0%
1 25.0%
1 25.0%
0 0.0%
0 0.0%
0 0.0%
0 0.0%
0 0.0%
0 0.0%
0 0.0%
0 0.0%
0 0.0%
0 0.0%
1 100.0%
0 0.0%
0 0.0%
0 0.0%
1 33.3%
0 0.0%
0 0.0%
1 33.3%
1 33.3%
0 0.0%
1 1.6%
1 1.6%
1 1.6%
0 0.0%
3 4.8%
1 1.6%
55 88.7%
0 0.0%
0 0.0%
1 10.0%
0 0.0%
0 0.0%
0 0.0%
0 0.0%
1 10.0%
8 80.0%
CCb
XT
D
K
L
ASa
S
V
Visible spectrum class

Particular case: V – types candidates

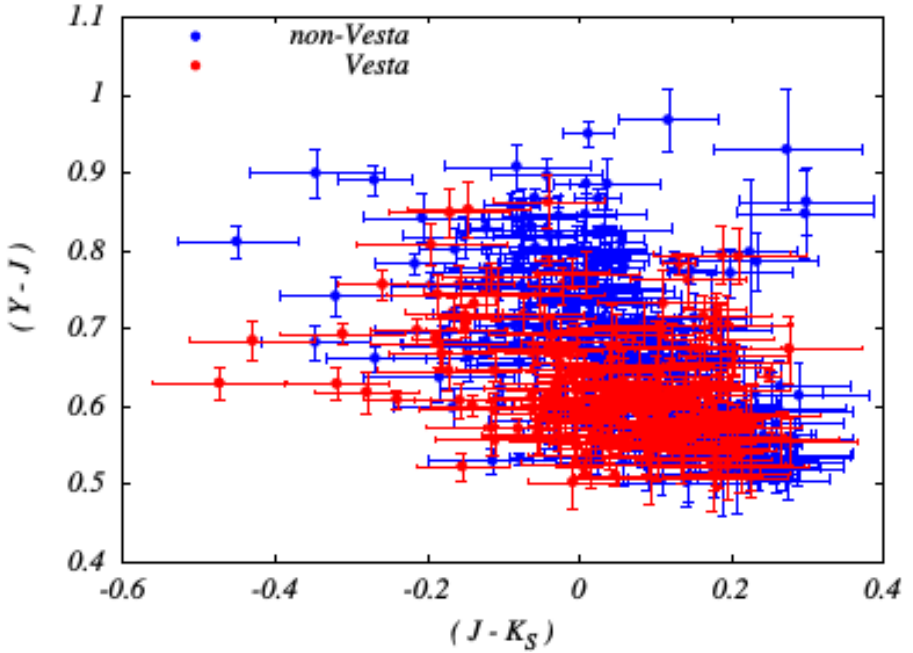

Colors distribution of the V-type candidates. Those with red belong to Vesta dynamicall familly

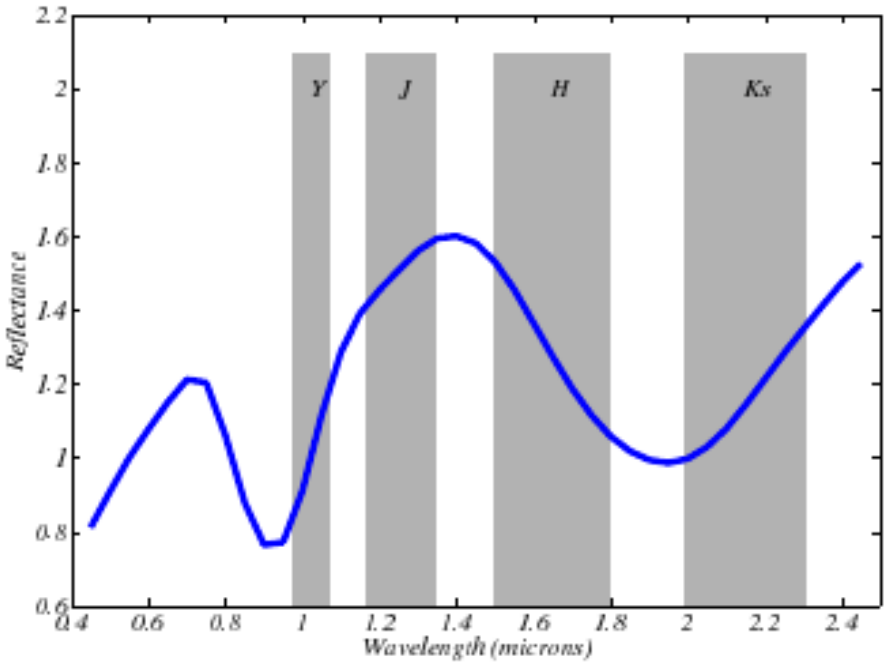

The template spectrum of a V-type asteroid the in Bus-DeMeo taxonomy.

- Basaltic asteroids are believed to be fragments of large bodies whose interiors reached the melting temperature of silicate rocks and subsequently differentiated. The discovery of the basaltic asteroids in the outer main belt challenged the models of the radial extent and the variability of the early Solar System temperature distribution, which generally do not predict melting temperature in this region.
- The asteroids with spectral properties similar with V type can be identified using Y-J-Ks filters - they appear as a separate group with large Y-J colour ($Y - J \geq 0.5$) and small J-Ks ($J - K_s \leq 0.03$). The group is also distinctive on the other colour-colour plot because it implies a step slope in the Y,J filters.

Licandro et al. (2017)

Case study: V-types identified by $(Y - J) \geq 0.5$ and $(J - K_s) \leq 0.3$

- We found 477 V-type candidates in MOVIS-C, 244 of them outside the Vesta dynamical family.
- We identified 19 V-type asteroids beyond the 3:1 mean motion resonance, and 16 V-types in the inner main belt with proper inclination ip ≤ 3.0º , well below the inclination of the Vesta family.
- We computed that ~ 85% of the members of the Vesta dynamical family are V-type asteroids, and only 2% are primitive class asteroids unlikely members of the family.

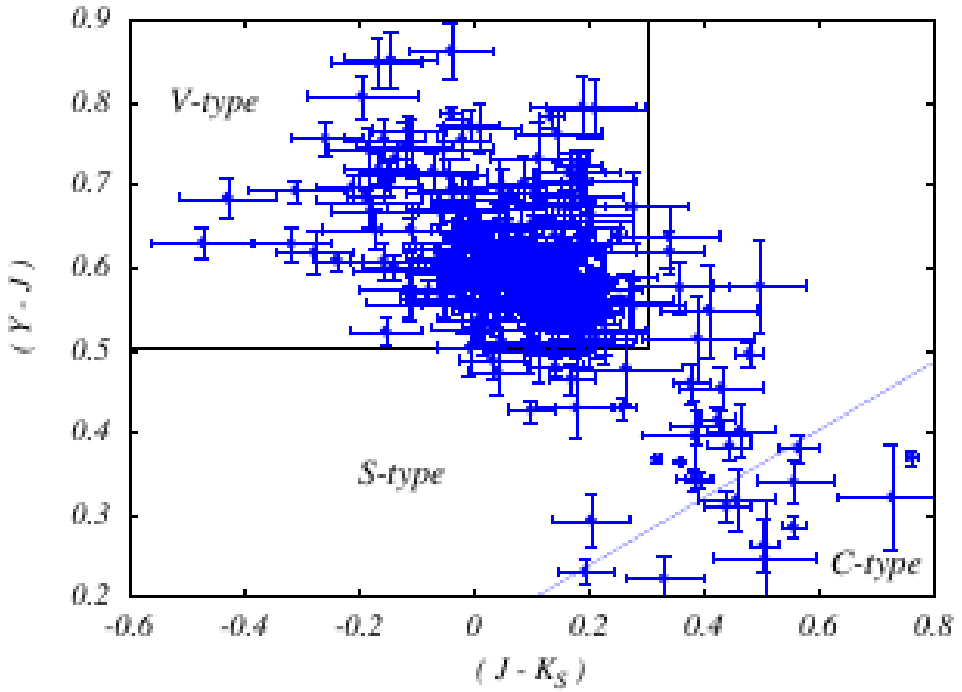

Colors distribution of the V-familly objects.

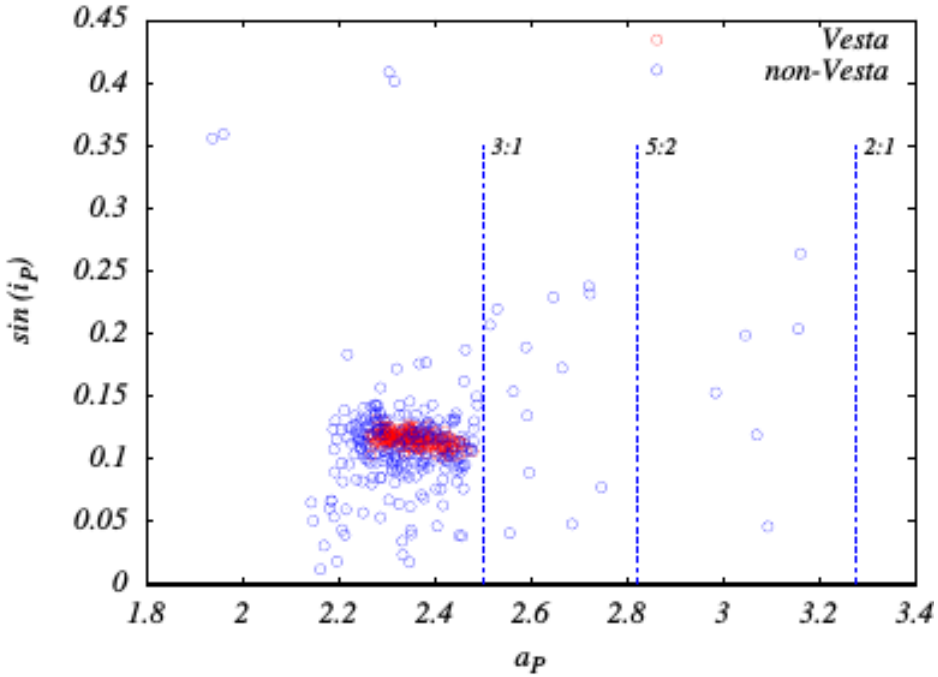

Distribution of V-type candidates in the proper orbital elements

Confirming the V – types with spectroscopy

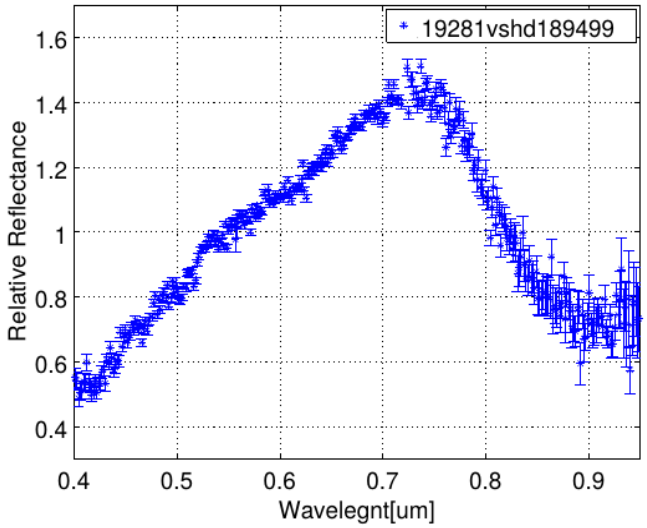

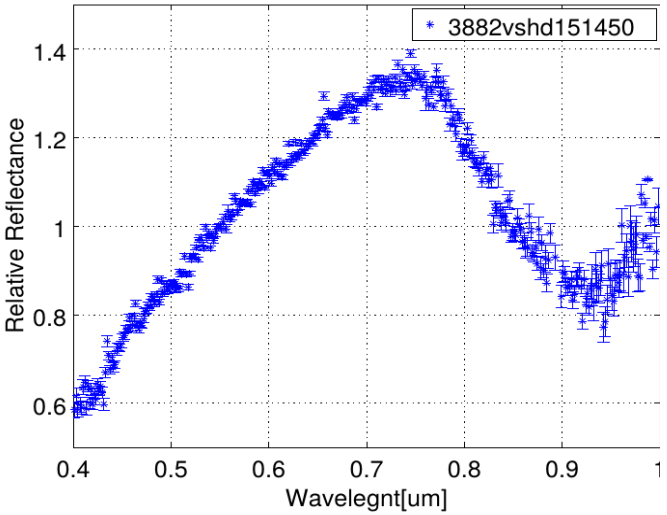

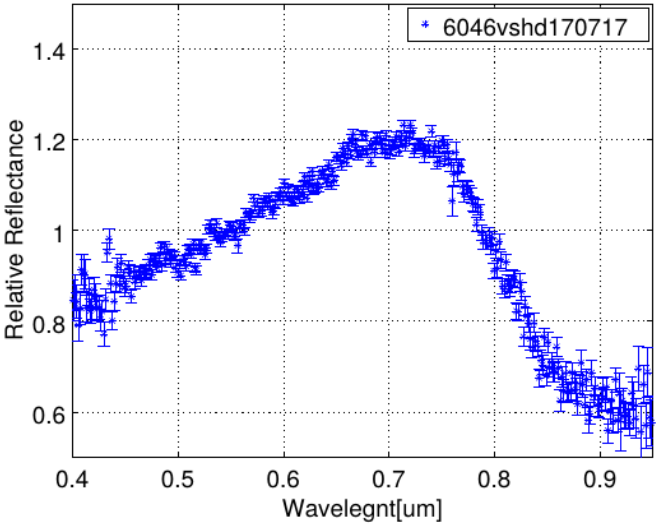

Visible spectra of some V-types candidates obtained with Isaac Newton Telescope – IDS instrument.

Number	Name	Y-J	Y-Jerr	J-K	J-Kerr	Albedo	aprop	eprop	siniprop
3882	Johncox	0.788969	0.006676	-0.081805	0.015464	0.3249	2.451128	0.136684	0.093296
6046	1991 RF14	0.793743	0.013918	0.037913	0.028457	0.1873	2.299685	0.109601	0.129168
19281	1996 AP3	0.857513	0.016897	-0.089056	0.037135	0.3158	2.28765	0.135711	0.133916

The “missing mantle problem”

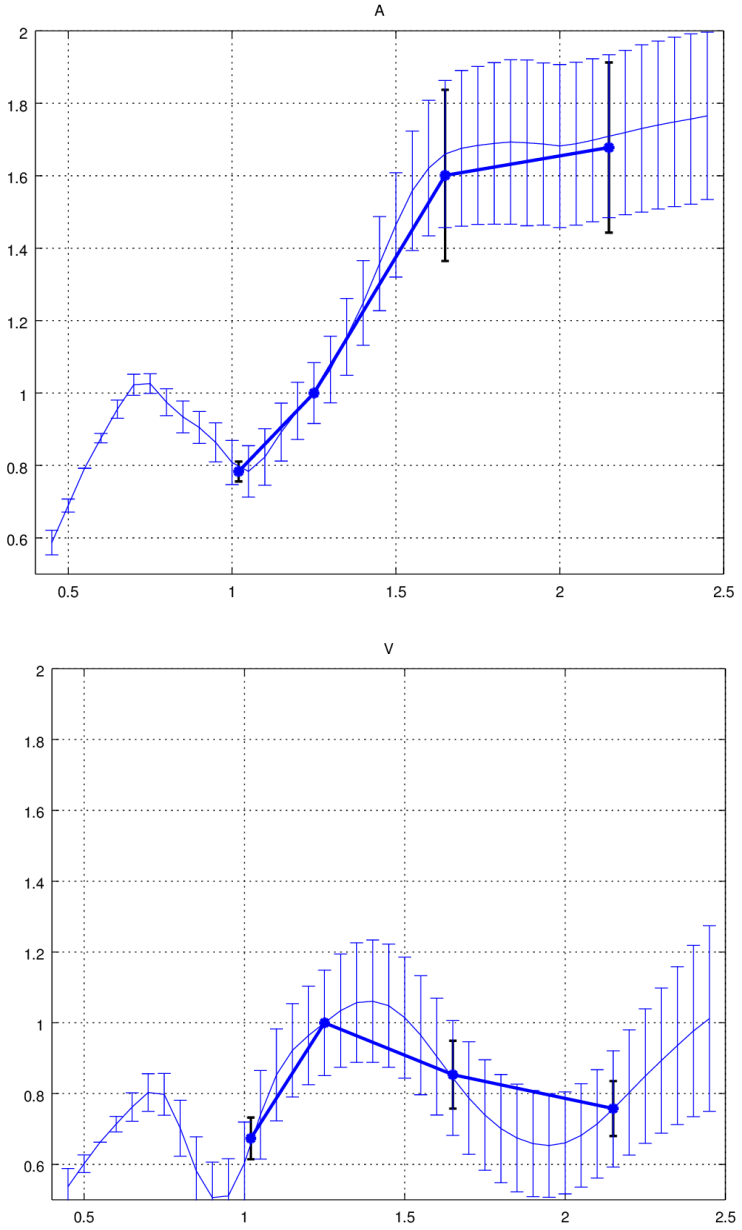

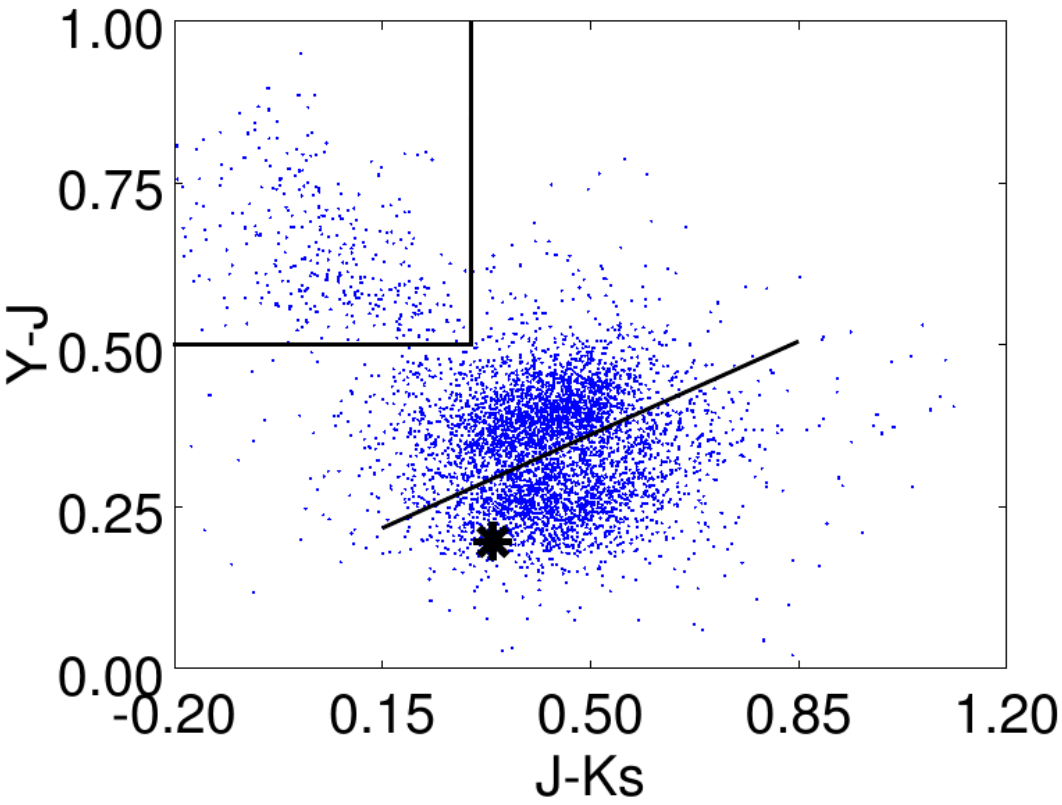

The “missing mantle problem”

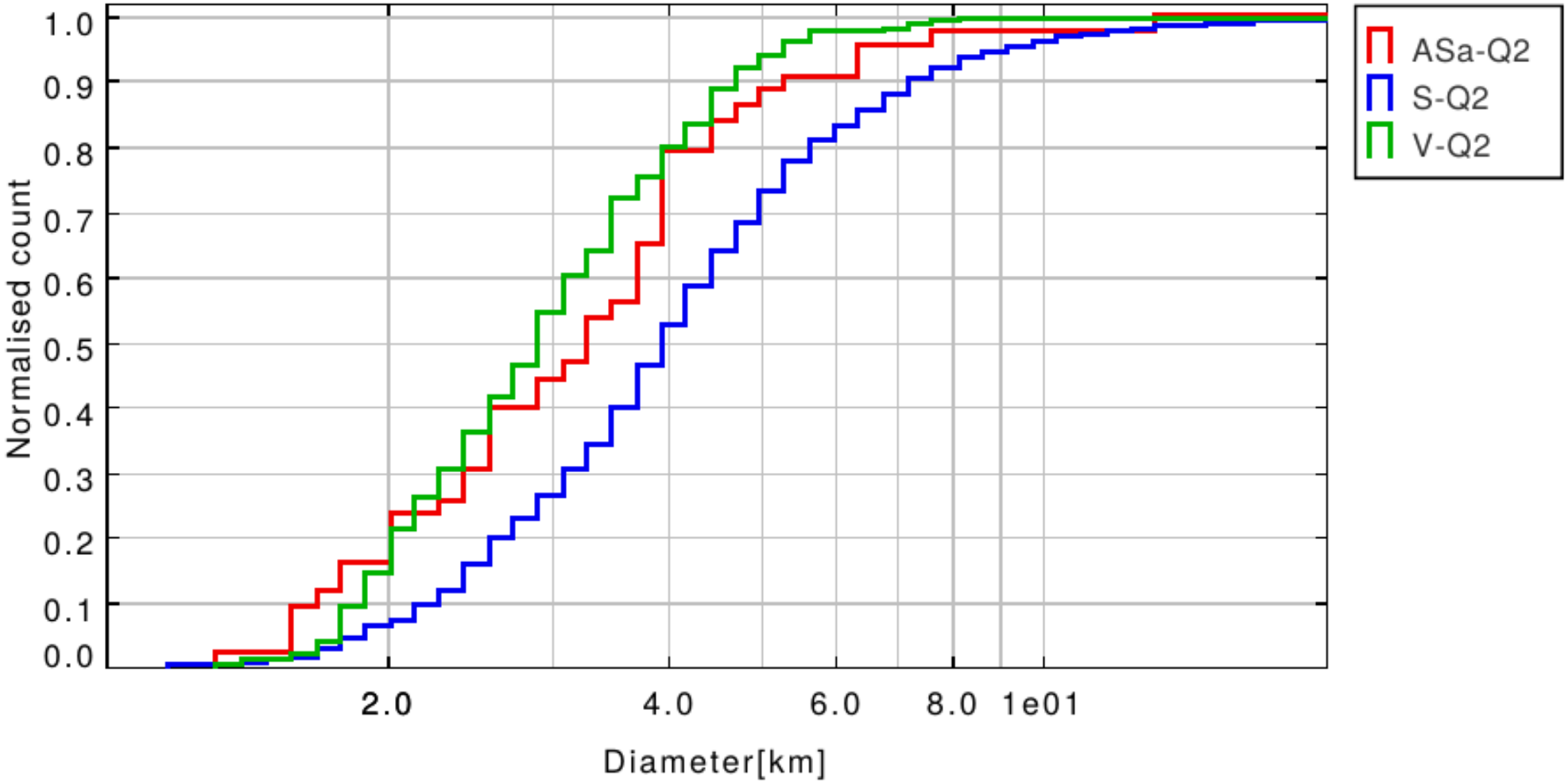

The “missing mantle problem”

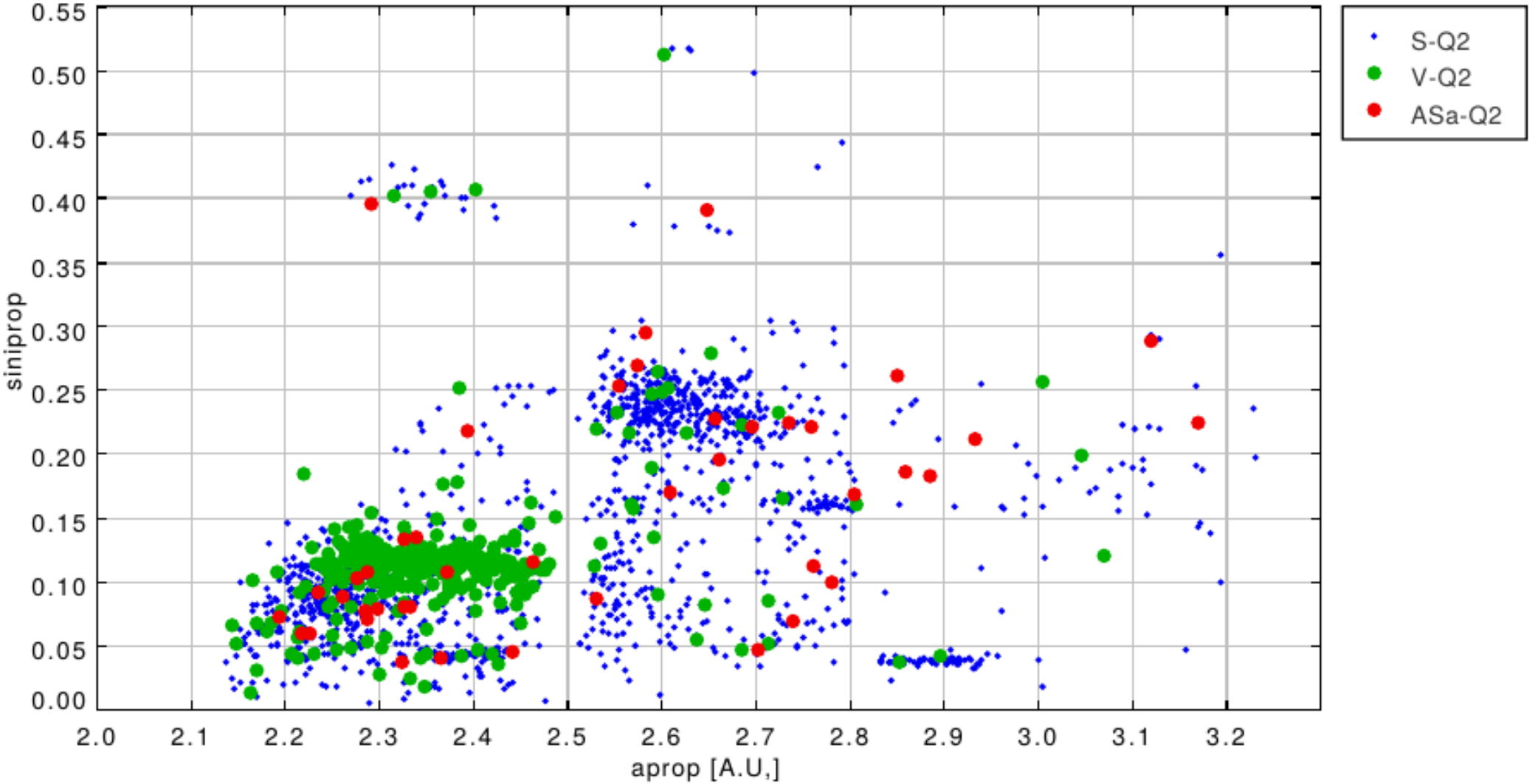

Conclusions

- ✔ The surface properties of an asteroid can be inferred through spectral and spectro - photometric measurements at wavelengths from the ultraviolet (UV) to the infrared.
- ✔ Spectral analysis for particular near-Earth asteroids has been shown
- ✔ A total of 39 947 SSo were detected in the VISTA VHS Data Release 3 (which covers ∼40% of the planned survey sky area). The detections found include: 52 NEAs, 325 Mars Crossers, 515 Hungaria asteroids, 38 428 Main Belt asteroids, 146 Cybele asteroid, 147 Hilda asteroids, 270 Trojans, 13 comets, 12 Kuiper Belt objects, and Neptune with its 4 satellites.
- ✔ The analysis of the near-infrared data shows the large diversity among different minor planets surfaces.
- ✔ All the diagrams that use (Y-J) color separate the spectral classes much better than it has been done until now using the (J-H) vs (H-Ks) plots.
- ✔ The MOVIS spectro-photometric provides new insights with respect to differentiation in the asteroid belt.